

## Conversion of the greenhouse gas CO<sub>2</sub> to the fuel gas CO via the Boudouard reaction: A review

Pooya Lahijani<sup>a</sup>, Zainal Alimuddin Zainal<sup>a,\*1</sup>, Maedeh Mohammadi<sup>b</sup>, Abdul Rahman Mohamed<sup>c,\*\*,1</sup>

<sup>a</sup> Biomass and Bioenergy Laboratory, School of Mechanical Engineering, Universiti Sains Malaysia, 14300 Nibong Tebal, Pulau Pinang, Malaysia

<sup>b</sup> Faculty of Chemical Engineering, Babol Noshirvani University of Technology, 47148 Babol, Iran

<sup>c</sup> Low Carbon Economy (LCE) Research Group, School of Chemical Engineering, Universiti Sains Malaysia, 14300 Nibong Tebal, Pulau Pinang, Malaysia



### ARTICLE INFO

#### Article history:

Received 4 April 2014

Received in revised form

18 July 2014

Accepted 17 August 2014

#### Keywords:

Boudouard reaction

CO<sub>2</sub>-char gasification

Activation energy

Char reaction rate

Char structural features

Kinetic study

### ABSTRACT

The remediation of carbon dioxide emitted into the atmosphere has become the topic of the day due to the enormous contribution of CO<sub>2</sub> to the devastating global warming. The Boudouard reaction, in which solid carbon (char) reacts with CO<sub>2</sub> to produce carbon monoxide (CO<sub>2</sub> (g)+C(s)↔CO (g)), is a straightforward route for the CO<sub>2</sub> emission mitigation. Through this reaction, the CO<sub>2</sub> coming from variety of combustion plants, including exhaust/flue gas and synthesis gas, can be upgraded to the fuel gas, CO. This work presents a review on the CO<sub>2</sub> gasification of char, from coal, biomass, municipal solid wastes, sewage sludge or any co-utilized blend of them, to produce CO through the Boudouard reaction. An outline of the most effective parameters on the char gasification rate is presented. The parameters which affect the char reactivity are reviewed as those related to the char and its structural features (surface area and porosity, active sites, mineral content, structural evolution of char during gasification, pyrolysis condition and carbon source) and operation parameters (use of catalyst, gasification temperature, gasification pressure and CO<sub>2</sub> partial pressure, char particle size and gasification heat source). The kinetics of the char gasification reaction is studied and several theoretical or semi-empirical kinetic models used to interpret the reaction rate data and calculation of kinetic parameters, specifically activation energy, are reviewed and discussed.

© 2014 Elsevier Ltd. All rights reserved.

### Contents

|   |     |
|---|-----|
| 1. Introduction.....  | 616 |
| 2. Factors affecting char reactivity .....                              | 616 |
| 2.1. Carbonaceous material and its characteristic features.....         | 617 |
| 2.1.1. Surface area and porosity .....                                  | 617 |
| 2.1.2. Active sites .....   | 617 |
| 2.1.3. Mineral content .....  | 618 |
| 2.1.4. Structural evolution of char during gasification .....           | 618 |
| 2.1.5. Pyrolysis condition .....  | 619 |
| 2.1.6. Carbon source .....  | 619 |
| 2.2. Effect of operation condition.....                                 | 620 |
| 2.2.1. Use of catalyst .....  | 620 |
| 2.2.2. Gasification temperature .....                                   | 621 |
| 2.2.3. Gasification pressure and CO <sub>2</sub> partial pressure ..... | 622 |
| 2.2.4. Char particle size .....   | 623 |
| 2.2.5. Gasification heat source.....                                    | 623 |

\* Corresponding author. Tel.: +60 4 593 7788; fax: +60 4 594 1025.

\*\* Corresponding author. Tel.: +60 4 599 6410; fax: +60 4 594 1013.

E-mail addresses: [mezainal@usm.my](mailto:mezainal@usm.my) (Z.A. Zainal), [chrahman@usm.my](mailto:chrahman@usm.my) (A.R. Mohamed).

<sup>1</sup> The two corresponding authors contributed equally to this work.

|   |     |
|---|-----|
| 3. Kinetics of char gasification reaction . . . . . | 624 |
| 4. Concluding remarks . . . . .                     | 629 |
| Acknowledgment . . . . .                            | 629 |
| References . . . . .                                | 629 |

---

## 1. Introduction

The introduction to global warming dates back to long before the industrial revolution; however, the over-indulgence in utilization of fossil fuel resources and massive release of greenhouse gases into the atmosphere has turned the term “global warming” to an inconvenient reality of modern life. The crisis of global warming will have a chilling perspective, if it could not be alleviated through rational strategies.

Carbon dioxide ( $\text{CO}_2$ ), although not the primary greenhouse gas, has had sizeable contribution to global warming. The global emission of  $\text{CO}_2$ , mostly emanating from fossil fuel combustion, reached a total of 34.5 billion tones in 2012; this accounts for 1.1% increase in  $\text{CO}_2$  emission which shows a reducing trend, as compared to an average annual increase of 2.9% since 2000 [1]. The slowing-down of the increase in anthropogenic  $\text{CO}_2$  emissions in 2012 reflects the decoupling of the long-standing relationship between the global economic growth and  $\text{CO}_2$  emission, which might point to the attitudes toward utilization of green and renewable energies and reducing demand on fossil fuel resources. Yet, the global average yearly growth in atmospheric  $\text{CO}_2$  concentration (2.45 ppm in 2012) is rather high [1]. The challenge of reducing carbon footprint cannot be tackled overnight and requires intellectual ventures to address the global warming crisis.

$\text{CO}_2$  remediation plants seek ways to develop long-term strategies for the remediation of this notorious greenhouse gas in the environment and scope to offer comprehensive solutions to climate change mitigation. Among the viable solutions, the reduction of  $\text{CO}_2$  to synthetically flexible and useful molecules seems most appealing. Nevertheless, the high thermodynamic stability of  $\text{CO}_2$  and its high oxidized status calls for highly efficient reductant, combined with a strong thermodynamic driving force to ensure irreversible reaction. A straightforward and well-known reaction for  $\text{CO}_2$  activation is the “Boudouard reaction”, wherein,  $\text{CO}_2$  is reacted with carbon to produce carbon monoxide:



The stoichiometry and reversibility of this reaction was first identified by Boudouard in 1899 [2]. This heterogeneous solutionless reaction is very important in gasification of carbonaceous materials and industrial smelting operations [3,4]. As indicated by the large positive enthalpy (172 kJ/mol at 298 K), Boudouard reaction is highly endothermic and the equilibrium lies far to the left to produce  $\text{CO}_2$  as the dominant product [5]. However, at high temperatures (typically  $> 700^\circ\text{C}$ ) [5,6] when the large positive entropic term ( $T \Delta S$ ) prevails the enthalpic component, the Gibbs free energy becomes negative ( $\Delta G = \Delta H - T \Delta S$ ) and the reaction proceeds spontaneously in forward direction to produce CO.

Use of  $\text{CO}_2$  as gasifying agent in gasification processes provides a reliable and long-term alternative to mitigate the accumulation of  $\text{CO}_2$  in the atmosphere and allows for production of clean fuels. Yet in another application, the quality of exhaust/flue gas, virtually coming from any industry, can be improved through the implementation of  $\text{CO}_2$ -char gasification as a post-treatment technique, whereby residual  $\text{CO}_2$  can be mostly converted to CO. Such processes incorporate  $\text{CO}_2$  into a valorization cycle to produce marketable fuels for various downstream applications, rather than capturing  $\text{CO}_2$  for sequestration.

The CO produced via the Boudouard reaction provides a chemical pathway for production of hydrogen through the water-gas shift reaction and synthesis of methanol and Fischer-Tropsch hydrocarbons in combination with  $\text{H}_2$ ; alternatively, CO can be utilized as carbonylation reagent in the synthesis of a number of chemicals [5,7].

This paper provides a review on  $\text{CO}_2$  gasification of char, virtually from any carbon-based material, and production of CO through the Boudouard reaction. An outline of the most influential parameters on char reaction rate is presented and different findings and conclusions in the literature are reviewed. The kinetics of the reaction under static (isothermal) gasification condition is studied and implementation of several kinetic models available in the literature to interpret the kinetic results and calculation of activation energy is discussed.

## 2. Factors affecting char reactivity

Research on the fundamental aspects of the gasification has explored the significance of char reaction rate with gasifying agent in controlling the overall performance of coal or biomass gasification [3,8–12]. The gasification reactivity of char with  $\text{CO}_2$  is even slower than that of  $\text{H}_2\text{O}$  and  $\text{O}_2$  [13]. Since the rate of this heterogeneous gas-solid reaction is much slower than the rate of other reactions involved in the gasification such as evaporation and devolatilization, char gasification is regarded as the rate controlling step in the gasification process [14–16]. The knowledge of the importance of char gasification rate to ultimate efficiency of gasifier and overall gasification performance and also as a decisive factor in the design process has become the subject of extensive research in this area and numerous studies have been undertaken to achieve higher char reactivity in the gasification. Generally, the reactivity of char during the gasification is known to be critically dependent on the type of carbon-based material to be gasified and its physicochemical properties as well as gasification condition such as reaction temperature, total pressure of the system, partial pressure of the gasifying agent, char particle size and heating rate. The char gasification reaction rate is defined as

$$r = \frac{dX}{dt} \quad (2)$$

$$X = \frac{w_0 - w}{w_0} \quad (3)$$

where  $X$  is the carbon (char) conversion,  $w_0$  and  $w$  are the initial and instantaneous mass of the char, both free from ash and  $t$  is the isothermal gasification time. However, different definitions of reaction rate or reactivity have been presented in the literature to evaluate the char reaction performance. Some works defined reactivity, also called specific reaction rate or instantaneous reaction rate, as

$$R = \frac{-1}{w} \frac{dw}{dt} = \frac{1}{1-X} \frac{dX}{dt} \quad (4)$$

In some other works, a reactivity index was defined to assess the overall gasification reactivity of char as

$$R = \frac{0.5}{\tau_{50}} \quad (5)$$

where  $\tau_{50}$  is the time required to reach the conversion of 50%. Nevertheless, many researchers did not discriminate between the reaction rate and reactivity and used them equivalently to describe the gasification reaction rate of char. The factors affecting char gasification reaction rate with  $\text{CO}_2$  are extensively discussed in the following sections.

### 2.1. Carbonaceous material and its characteristic features

Any gasification reaction typically consists of two major steps: (1) initial rapid pyrolysis of carbon-based material and (2) the subsequent gasification of the resultant char [14,15,17]. The heat treatment of carbonaceous material (coal, biomass, mixed coal, biomass, etc.), results in evaporation of moisture and devolatilization of hydrocarbons and gases, which substantially contribute to pyrolysis reaction during the gasification process. The resultant char then reacts with gasifying agent to produce gaseous fuel. However, it is worth noting that, the properties of this char (produced during the gasification of carbonaceous material with reactive medium) is very different from the char produced under an inert environment and consequently subjected to the gasification [18]. Unless specified otherwise, all the works reviewed in this paper separate the pyrolysis and char gasification reactions.

#### 2.1.1. Surface area and porosity

The reaction rate of char is known to be affected by the magnitude and accessibility of surface area, where the heterogeneous reaction of carbon with gas takes place during char gasification [19]. The gasification reaction rate might be proportional to the specific surface area and pore volume of the char; however, there is not a definite consensus among researchers about the influence of these microstructural properties. In an attempt to define a correlation between the surface area (as determined by BET analysis) of char and its reactivity in the gasification, Scott et al. [20] gasified three chars, derived from dried swedge sludge, car tire and bituminous coal, and a high surface area activated carbon with  $\text{CO}_2$ . They deduced that the reactivity of chars did not correlate with corresponding surface areas, where the reactivity of activated carbon with massive surface area was an order of magnitude slower than coal char signifying that the microporous surface area of activated carbon was comparatively unreactive in gasification. Xu et al. [21] also did not see good correlation between the BET surface area of several coal char samples, prepared under different pyrolysis conditions, and their gasification reactivity. However, Duman et al. [22] could observe a relation between surface area and reactivity of several biomass chars in  $\text{CO}_2$  gasification, where the larger the BET surface area of char, the higher was the char reactivity. This proportionality between surface area and char reactivity was also reported by Vamvuka et al. [23], while gasifying the chars from municipal solid waste (MSW), sewage sludge and waste paper; the highest  $\text{CO}_2$  gasification reactivity was obtained with waste paper char with highest surface area. In another investigation undertaken by Kim et al. [14], the gasification reactivity of chars prepared from 12 bituminous coals were compared in  $\text{CO}_2$  gasification. They observed that the reactivity of chars was more correlated with mesopore volume than with the specific surface area and this relevance of reactivity to mesopore volume was more pronounced at higher gasification temperatures. Yet, a different observation was reported by Sakawa et al. [24] who examined the influence of coal characteristics on  $\text{CO}_2$  gasification and found that the gasification rate of coke was not dependent on total volume of pores in the coke. In another study performed by Hurt et al. [25], the role of microporous surface area of coal chars in the  $\text{CO}_2$  gasification was considered. There were evidences in their work

that the microporous surface area of the char did not contribute to the char reactivity and the reaction occurred outside the microporous network. The possible mechanism for limited participation of micropores in the reaction could be the restricted diffusion of  $\text{CO}_2$  into the micropores during the limited time for reaction. However, they pointed to the role of microporous area in catalytic char gasification, where the surface area provides a means for dispersion of catalytic elements. In brief, it can be concluded that the reaction rate of char is proportional to the number of active sites on the surface for heterogeneous gas-solid reaction, rather than total surface area of the char [26].

#### 2.1.2. Active sites

Several physicochemical properties of char are known to affect the char reactivity; among which, the concentration of active sites might be considered as the underpinning parameter that determines the char reactivity [21]. Char consists of polynuclear aromatic structures which are inert during gasification. However, the edge carbons, the carbon atoms bonded to heteroatoms and the nascent sites which are attached to aromatic clusters are at least an order of magnitude more reactive than the carbon atoms and thus are considered as carbon active sites [21,27]. These carbon active sites differ from catalytic active sites which represent the catalytic activity of minerals in the char (see Section 2.1.3). The proportionality of the number of active sites in the char to the reactivity of char and progress of the Boudouard reaction can be better understood through the mechanism of the reaction. The most widely used mechanism to describe the  $\text{CO}_2$  gasification reaction is the oxygen-exchange mechanism which has been proposed by Ergun [28,29]:



where  $\text{C}_f$  denotes the free carbon active site and  $\text{C}(\text{O})$  represents the reactive carbon-oxygen surface complex; it represents an occupied site. Based on this mechanism,  $\text{CO}_2$  is first dissociated at a free carbon active site through which a reactive surface complex of carbon-oxygen and a molecule of CO are created [28,30]. In the next step, the carbon-oxygen complex produces a new vacant active site and another molecule of CO. Indeed, reaction (6) expresses the oxygen-exchange phenomenon and reaction (7) illustrates the transfer of carbon from solid phase to gas phase [28]. This mechanism signifies that the number of active sites plays a critical role in char reactivity in  $\text{CO}_2$  gasification. Yet, there is not a universal measurement method to evaluate the number of active sites. Some investigations demonstrated that the gasification reactivity of char can be associated with the active surface area of char which is determined by  $\text{CO}_2$  chemisorption at 300 °C. Molina et al. [31] implemented a conventional volumetric  $\text{CO}_2$  chemisorption unit to characterize the active surface area of coal char. Based on their method, it was possible to differentiate between strong  $\text{CO}_2$  chemisorption (irreversible) and weak  $\text{CO}_2$  chemisorption (reversible) and it was proposed that the strong chemisorption could be a reliable value of the active surface area. However, Jing et al. [13] pointed that volumetric chemisorption method might not be that much accurate, as the volume of  $\text{CO}_2$  chemisorbed by coal char is extremely small. They used thermogravimetric analyzer (TGA) as an ideal instrument for measuring the  $\text{CO}_2$  chemisorption of char and used it as an index to compare the  $\text{CO}_2$  gasification reactivity of eight different coal rank chars. In  $\text{CO}_2$  chemisorption test, total ( $\text{C}_{\text{total}}$ ), strong ( $\text{C}_{\text{strong}}$ ) and weak ( $\text{C}_{\text{weak}}$ ) chemisorbed volumes were obtained and it was found that  $\text{C}_{\text{total}}$  and  $\text{C}_{\text{strong}}$  were good indexes to evaluate the gasification reactivity of different coal ranks. They also concluded that the volume of  $\text{CO}_2$  chemisorption can be affected by the alkali index,

pore and carbon crystalline structure of the char. Xu et al. [21] also carried out similar CO<sub>2</sub> chemisorption experiment on several char samples obtained from slow and fast pyrolysis of coal. They found that C<sub>strong</sub> and C<sub>weak</sub>, respectively related to the presence of active inorganic minerals and organic matter of char, were better parameters to explain the char reactivity, rather than BET surface area. Similar CO<sub>2</sub> chemisorption tests were conducted by Zhang et al. [32] on potassium and calcium catalyzed coal char or carbon. It was shown that addition of K and Ca led to significant increase in irreversible CO<sub>2</sub> chemical uptake signifying that alkali metal could contribute to increase the concentration of active sites on the char or carbon surface.

### 2.1.3. Mineral content

The overall gasification reaction may be considered as a combination of non-catalytic process and catalytic process associated with mineral content of the char. Thus, the overall gasification rate can be influenced by both the catalytic and non-catalytic gasification rates. The rate of non-catalytic gasification is known to be influenced by the physicochemical properties of the char; while, the rate of catalytic gasification is controlled mainly by the alkali and alkaline earth metal in the char [33]. It is worth noting that the latter is predominant in low rank coal and biomass chars gasification [33,34].

As prior mentioned the reaction of carbon–CO<sub>2</sub> is an endothermic and slow process, where catalytic species are required to speed up the reaction rate at temperatures below 900 °C [35]. Alkali and alkaline earth metals are individually known as good catalysts for char gasification; whereas, Si and Al play an inhibiting role [13,21]. The presence of SiO<sub>2</sub> and Al<sub>2</sub>O<sub>3</sub> in the char reduces the reactivity of char, as they react with elements in the ash and create different inactive complex silicates including K, Na, Ca, Mg and Fe elements [36–38]. To quantify the catalytic effect of minerals available in the ash of carbonaceous material on promoting the char reactivity, the alkali index is defined as [14,24,39]:

$$\text{alkali index} = \text{ash content (wt\%)} \frac{\text{Fe}_2\text{O}_3 + \text{CaO} + \text{MgO} + \text{Na}_2\text{O} + \text{K}_2\text{O}}{\text{SiO}_2 + \text{Al}_2\text{O}_3} \quad (8)$$

The alkali index is the ratio of the sum of the mass fractions of alkali compounds in the ash to the sum of the mass fraction of acid compounds, multiplied by the ash content of the carbon-based material. The mostly encountered pattern reported by many researchers is the presence of good correlation between alkali index and gasification reactivity, where with increase of the alkali index, the gasification reactivity of char improves [14,24,40].

To explore the catalytic effect of inherent alkali/alkaline earth metals available in carbonaceous feedstocks, acid washing is usually implemented as the most common process to eliminate the inherent mineral matters from the biomass or coal under investigation [41]. With this knowledge, Duman et al. [22] compared the gasification reactivity of several raw and acid-washed biomass chars in CO<sub>2</sub> gasification. Acid washing substantially removed K and Ca from the chars and led to remarkable decrease in gasification reactivity. They also concluded that surface area of chars had a higher contribution to char reactivity compared to indigenous mineral matter. In another investigation performed by Zhang et al. [39], the catalytic effect of the inherent minerals on the gasification reactivity of six anthracite chars was considered. Although the chars with higher alkali index showed higher reactivity, however, when the chars were demineralized the observed trend for char reactivity in CO<sub>2</sub> gasification was unexpected. Two of the demineralized chars showed a lower reactivity compared to the corresponding raw chars and four of the demineralized chars revealed higher reaction rate compared to the corresponding pristine chars. It was speculated that the observed

higher reactivity of the demineralized chars was attributed to the enhancement of surface area and pore enlargement during demineralization (acid-washing) process. It should be noted that since the char gasification, as a heterogeneous gas–solid reaction, is a surface-initiated process, both the dispersion of minerals and availability of active sites can contribute to enhance the gasification reactivity [35]. Although many researches pointed to the direct relation of alkali index (not in exact word) and the gasification reactivity of char [17,25,42]; yet, a different behavior was reported by Lin and Strand [43], who compared the CO<sub>2</sub> gasification reactivity of eight char samples from wood, miscanthus and straw. Although the chars from straw and miscanthus contained higher amount of alkali metals, they presented lower gasification reactivity. As a plausible explanation, they mentioned the high silicon content in the two chars, which could contribute to the lower reactivity. Another related aspect, based on their experimental observation, could be the higher ash content of the two chars, where the ash always contained some black matter and it was speculated that the high ash content caused pore blockage and hindered the char reactivity. Hattingh et al. [40] also compared the catalytic effect of inorganic species in the ash of three coal samples and found an inverse relation between ash content and CO<sub>2</sub> gasification reactivity of coal char. It was deduced that the char reactivity was not solely dependent on ash content, but also depends on inherent mineral matters in the ash. The highest gasification reactivity was devoted to the coal char with highest amount of CaO and MgO and lowest amount of non-catalytic SiO<sub>2</sub>. The inherent catalytic effect of K<sub>2</sub>O and Na<sub>2</sub>O on promoting the char reactivity was negligible due to their low concentrations in the ash. On the contrary, the coal char sample with highest amount of ash, but also highest SiO<sub>2</sub> content showed the lowest reactivity. It was explained that at high gasification temperatures, the melting of alumina-silicates and silicates could cover the available active sites or block the pores within the coal char particles and thus hindered the carbon conversion rate. In another effort to study the dependence of gasification rate on the indigenous metal content, Kannan and Richards [35] compared the reaction rate of ten different biomass samples with diverse natural metal ions contents. A linear correlation was found between the combined molar concentrations of K and Ca with gasification reactivity, except for two samples which contained the highest amount of Si. It was also found that the catalytic effect of K was diminished though the reaction with Si to form silicate; however, it was not the case for Ca and its catalytic effect was not significantly affected in the presence of Si.

### 2.1.4. Structural evolution of char during gasification

Understanding the structural features of char and its evolution during gasification provides useful information for development of gasification-based systems. Several advanced instrumental techniques such as X-ray diffraction (XRD), NMR, FTIR and Raman spectroscopy have been implemented to investigate the structural features of carbon or char. XRD analysis is used to characterize the crystalline structure of carbon materials such as polycrystalline graphite structure. NMR spectroscopy has been implemented to identify different char structures including aliphatic and aromatic carbons and oxygen-containing carbon groups. FTIR spectroscopy is a useful analysis to detect various oxygen-containing functional groups. Raman spectroscopy has been implemented as a powerful tool to analyze the structural features of chars obtained from pyrolysis and gasification of carbonaceous materials, in which, D band (reflecting disordered or defect structure) and G band (reflecting graphite structure) are assigned [11,16,34,44].

Evolution of char structure during the CO<sub>2</sub> gasification in terms of changes in pore surface area, carbon crystalline structure and

inherent alkali and alkaline earth metal (AAEM) content has been investigated by some researchers. Tancredi et al. [45] reported that the reactivity of chars obtained from eucalyptus wood monotonically increased with conversion in CO<sub>2</sub> gasification. It was inferred that the enhanced reactivity at low and intermediate conversions was attributed to the enlargement of surface area, as the reaction proceeded, where CO<sub>2</sub> reaction led to the widening of micropores and increased the contribution of meso- and macropores in providing accessible surface area. At high conversions, however, the increase in reactivity was steeper and probably attributed to the catalytic effects offered by inorganic constituents, especially K and Na, whose proportion in the solid residue increased with burn-off and their catalytic role became significant. Similar observation and discussions regarding development of surface area and catalytic activity of inherent inorganic matter with progress of gasification have been presented by Marquez-Montesinos et al. [46] in CO<sub>2</sub> gasification of grapefruit skin char. They further confirmed the catalytic activity of inorganic matters by lowering the ash content of char through acid-washing; where, the acid-washed char presented considerably lower reactivity than the original char. Jing et al. [47] studied the gasification reactivity of several coal char samples, considering the structural evolution of chars during the CO<sub>2</sub> gasification. In all cases, it was observed that the gasification rate profile experienced a maximum and then gradually declined with carbon conversion. It was deduced that the initial increase in the reaction rate was attributed to the variation of pore structure during gasification and opening of the blocked pores at the initial stage of the gasification, followed by widening of micropores. Nevertheless, as the reaction proceeded, coalescence of neighboring pores and destruction of the macropores lowered the reaction rate in accordance to the reduction in surface area. They also discussed that, although inorganic constituents, especially the AAEMs, offered catalytic effect in char gasification reaction, however, with increase of the carbon conversion, the share of ash in the carbonaceous material increased and the ash layer became thickened. This could possibly inhibit the diffusion of CO<sub>2</sub> into the pores at high conversions and hence reduced the reaction rate. Gil et al. [48] prepared several plastic waste char samples with different degrees of burn-off and used them in the CO<sub>2</sub> gasification tests. They determined the BET and micropore surface area of the samples using N<sub>2</sub> adsorption isotherms and the narrow micropore surface area using CO<sub>2</sub> adsorption isotherms. Although the surface area (N<sub>2</sub> BET, N<sub>2</sub> micro, CO<sub>2</sub> narrow micro) of the chars changed with conversion, however, the ratio of the reaction rate to the narrow micropore surface area remained constant with conversion. Thus, the narrow micropore surface area was found to be a good parameter for describing the CO<sub>2</sub> gasification reactivity of the plastic chars. It was also concluded that the reaction rate was controlled by the narrow microporosity during the gasification and that such surface area can be considered as the surface area available for the gasification reaction.

### 2.1.5. Pyrolysis condition

For a given carbon-based material and a specific gasification condition, the char reactivity in the gasification process has been recognized to be mainly influenced by the char thermal history and many parameters involved in the pyrolysis of the raw carbonaceous material. The structural evolutions of char during pyrolysis, which refers to the loss of surface functional groups, rearrangement of the carbon microstructure to become more graphitic and volatilization of inorganic materials acting as catalytic active sites under heat treatment, contribute to the decrease of char reactivity in gasification reaction [21]. Numerous studies are found in the literature extensively discussing the effect of

pyrolysis condition (such as temperature, heating rate, particle size etc.) on the produced char characteristics with relatively good agreement among researchers [16,17,49–51]. Min et al. [17] investigated the effect of pyrolysis temperature on the CO<sub>2</sub> gasification reactivity of two biomass chars. It was found that with decrease of the pyrolysis temperature the gasification reactivity of chars improved. Although high pyrolysis temperature created chars with many small pores, thinner cell walls and larger surface area, however, the char gasification reactivity decreased due to the difficulties in access of CO<sub>2</sub> to microporous structure of chars to react with char surface. They concluded that the gasification reactivity of the chars correlated well with the pyrolysis temperature. These results are consistent with findings of Yuan et al. [52] who found that increase of the pyrolysis temperature decreased the gasification reactivity of three biomass derived chars, due to the increase of uniformity and graphitization degree of chars with increase of temperature. Similar proportionality has been reported by Fermoso et al. [29] who reported that the CO<sub>2</sub> gasification reactivity of wood char decreased with increase of pyrolysis temperature, probably attributing to the ordering of carbon matrix and reducing the concentration of active sites. Generally, rapid pyrolysis and high heating rates create char with larger surface area and higher concentration of active sites and thus contribute to the higher reactivity of char during the gasification [13]. In this regard, Luo et al. [53] investigated the CO<sub>2</sub> gasification reactivity of coal char samples pyrolyzed under rapid and slow heating conditions. The results showed that the reaction rate for high-volatile bituminous coal char prepared under rapid pyrolysis was several time higher than that of slow pyrolysis; however, for medium-volatile bituminous coal, the heating rate was not that much significant. Analysis of porosity and specific surface area revealed that higher reaction rate of chars obtained under rapid pyrolysis was attributed to the higher porosity and that the effect of heating rate became greater with increase in volatile matter. Xu et al. [21] also reported that implementation of high pyrolysis temperature and slow heating rate enhanced the C/H and C/O mole ratios in the coal char, improved the crystalline structure of the char and reduced the active mineral compounds in the char and as a consequence, the concentration of surface active sites decreased.

### 2.1.6. Carbon source

For chars from different sources, several physicochemical properties of char take part in CO<sub>2</sub> gasification reactivity. The physicochemical properties of char depend deeply on the utilized carbonaceous feedstock. A vast variety of carbon-based materials including coal, biomass, lignite, graphite, municipal solid waste, sewage sludge and many other carbon-containing materials have been used to prepare char for CO<sub>2</sub> gasification. Considering the great differences among these feedstock materials in terms of fixed carbon, volatile matter and ash content, the subsequent differences in char reactivity would be expected. Such differences are reflected in the gasification of chars derived from lignocellulosic biomass materials compared to coal derived chars. The volatile content of biomass fuel is known to be at least twice that of coal [49]. The higher yield of volatile in biomass reveals the strong effect of thermal treatment on depolymerization reaction which concludes to the rapid evolution of volatile matters; whereas, the lower release of volatile during pyrolysis of coal is an indication of strong bonding within the coal structure [54,55]. As another difference, biomass fuels typically have less aluminum and iron and more silica and potassium and sometimes calcium than coal [56]. The higher content of volatile matter in biomass beside inorganic properties of biomass fuel (which might exert catalytic effect) contributes to its higher reactivity compared to

coal in pyrolysis, combustion and gasification process [56]. Some works noted the higher reactivity of chars derived from materials with higher volatile matter, due to the evolution of surface area and development of pore structure during devolatilization and thus higher concentration of active sites in the char matrix [14,57]. This is the case mostly observed while gasifying low rank coal (high volatile matter) chars compared to high rank ones (low volatile matter), where low rank coal chars are more reactive than high rank coal chars, except for graphite [58].

Co-gasification has been proposed as an alternative to improve the char reactivity and gasification rate of materials with low reactivity. The synergistic effects occurring during co-gasification of biomass and non-biomass feedstock is known to be beneficial with respect to char reactivity and greenhouse gas emissions [59,60]. The promoting effect of biomass on the gasification reactivity of char blends in co-gasification process is attributed to the alkali (K, Na) and alkaline earth metals (Mg, Ca) content of biomass, especially in herbaceous type of biomass, originating from the nutritional requirements of plants during growth process [60,61]. In an effort to enhance the gasification reactivity of char through co-gasification, Habibi et al. [60] gasified blends of sub-bituminous coal–switchgrass and fluid coke–switchgrass. Switchgrass was used as a biomass rich in potassium and it was explained that the intraparticle mobility of potassium allowed the transfer of catalyst from biomass to the second feedstock. CO<sub>2</sub> co-gasification of biomass with sub-bituminous coal (with high ash content) imposed an inhibitory effect on the gasification reaction probably due to the formation of inactive alkali aluminosilicates. However, in co-gasification of biomass and fluid coke (with low ash content), where little interfering inorganic matter presented, the gasification rate was enhanced. Similar promoting effect of biomass on char gasification reactivity was reported by Brown et al. [59] in co-gasification of switchgrass and coal chars and Zhu et al. [61] in gasification of chars obtained from co-pyrolysis of coal and wheat straw. In another investigation conducted by Jeong et al. [62], reactive synergy was observed in co-gasification of coal and pine sawdust which increased with the amount of utilized biomass, due to the catalytic effects offered by alkaline minerals in the biomass. However, Kajitani et al. [63] did not observe neither distinguished synergistic nor inhibition effect on the gasification reactivity of cedar bark and coal blend in high temperature CO<sub>2</sub> gasification; nevertheless, a little improvement in reactivity was observed in low temperature co-gasification. Beside co-gasification of coal and biomass, co-utilization of tire derived char and biomass has also been implemented to improve the gasification reactivity of tire char. Although the heating value of tire is higher than that of biomass and coal [64], however, tire char presents very low reactivity in gasification [65,66]. In this regard, Lahijani et al. [42] co-utilized tire–palm empty fruit bunch and tire–almond shell blend chars in CO<sub>2</sub> gasification and observed remarkable enhancement in the char reactivity, especially in the case of palm empty fruit bunch. The pronounced influence of inherent alkali content of biomass materials, which were rich in potassium, on improvement of tire char reactivity was proved, when acid-washed biomass chars did not offer any catalytic effect to enhance the tire char reactivity in co-gasification.

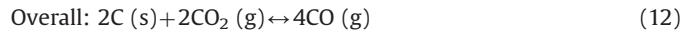
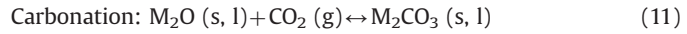
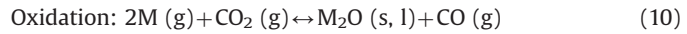
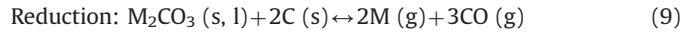
## 2.2. Effect of operation condition

### 2.2.1. Use of catalyst

Very often, the natural surface chemistry of char is not potent enough to encourage the heterogeneous gas–solid reactions. In such case, incorporation of the desired heteroatoms within the char framework would modify the carbon surface chemistry and enhance its physicochemical properties, which eventually contribute to the higher gasification reactivities [67]. Addition of catalyst

to the carbon material which is subjected to gasification is a promising route to reduce the reaction temperature significantly [68–71], thus mitigating the severity of the reactor condition and the cost of the gasification process. It also provides a selective reaction pathway towards the production of the desired product [72]. Although it has been suggested that the catalyst only increases the number of active sites without changing the chief kinetic mechanism [31,73], it has also been proposed that the catalyst alters the identity and reactivity of the surface intermediates [73].

A number of researches have been conducted implementing alkali, alkaline earth and transition metal salts and oxides to catalyze the gasification reaction of a range of carbonaceous materials. Huang et al. [74] studied the effect of alkali (K and Na), alkaline earth (Ca and Mg) and transition (Fe) metals on the CO<sub>2</sub> gasification reactivity of fir char and found the catalytic effect of the metals in the order K > Na > Ca > Fe > Mg. It was speculated that the increase in char reactivity in the presence of catalyst was attributed to the increase of reaction centers which play a critical role in progress of the reaction. Kopyscinski et al. [75] studied the kinetics of K<sub>2</sub>CO<sub>3</sub>-catalyzed ash-free coal in CO<sub>2</sub> gasification. It was reported that the gasification rate of ash-free coal dry mixed with 20% K<sub>2</sub>CO<sub>3</sub> was about 3 and 60 times faster than that of pristine coal and ash-free coal. It was also found that increase of the catalyst amount from 20% to 45%, increased the gasification rate 3-fold. The mechanism through which the alkali metals catalyze the Boudouard reaction was suggested to involve gaseous intermediate compounds M (g), CO (g) and CO<sub>2</sub> (g), where M (g) represents K, Li, Na, etc. [76]. The mechanism involves the following reactions:



Reaction (9) was speculated to be the rate controlling step, while, the reactions (10) and (11) were expected to proceed rapidly. Rao et al. [76] also reported that at temperatures above the melting point of K<sub>2</sub>CO<sub>3</sub>, the catalytic activities were in the order of K<sub>2</sub>CO<sub>3</sub> > Na<sub>2</sub>CO<sub>3</sub> > Li<sub>2</sub>CO<sub>3</sub>. In another work by Alam and Debroy [77] same vapor cycle mechanism was adopted for gasification of Na<sub>2</sub>CO<sub>3</sub> catalyzed coke. They also emphasized that it was unlikely that reaction (10) control the overall reaction rate, as Na (g) is highly active.

Calcium has been used as a potential catalyst for promoting the char gasification reaction. Although its catalytic activity is inferior to that of potassium, however, it shows low agglomeration tendency and volatilization during gasification [36,78]. This might be considered as the main advantage of Ca over K and Na, which are mobile and volatile at gasification temperature and show high tendency to form low melting eutectics in the presence of silica (especially in the case of biomass char) and cause sintering and agglomeration [36,79]. However, catalytic activity of Ca is remarkable only when it is well dispersed to active sites in the carbon matrix. To this end, Zhang et al. [80] implemented an oil-slurry dewatering process, as a novel method over conventional impregnation and ion-exchange methods, for Ca loading on coffee ground. They found dewatering process as an effective method for even loading of catalyst on biomass fuels with high water content. The catalytic activity of 3% Ca loaded char obtained by this method in the gasification reaction was comparable to that prepared by impregnation method. Mitsuoka et al. [81] studied the influence of K and Ca on the CO<sub>2</sub> gasification reactivity of Japanese cypress (hinoki) char. The reactivity of the char enhanced

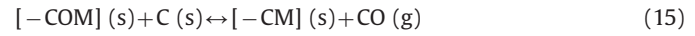
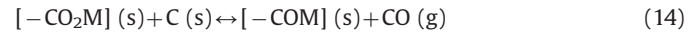
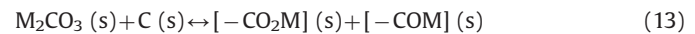
in the presence of these metals, with Ca-char leading that of K-char. It was hypothesized that since Ca and K were loaded on the char by two different methods, their dispersion on the char surface was probably different which could definitely affect the gasification rate.

Iron species with almost unlimited availability have been used as promising catalysts for enhancing the Boudouard reaction rate. In this regard, Zhou et al. [68] compared the catalytic effect of  $\text{FeCl}_3$ ,  $\text{FeSO}_4$  and  $\text{Fe}(\text{NO}_3)_3$  on  $\text{CO}_2$  gasification reactivity of petroleum coke. They reported the catalytic activity of iron species in the order of  $\text{FeCl}_3 > \text{Fe}(\text{NO}_3)_3 > \text{FeSO}_4$ . It was also reported that the catalytic effect of  $\text{FeCl}_3$  improved through addition of  $\text{Ca}(\text{OH})_2$  to obtain Cl-free iron catalyst, as Cl-containing compounds can pose serious problems to the gasification systems. Asami et al. [69] also reported the marked catalytic effect of the iron catalyst which was precipitated from  $\text{FeCl}_3$  solution using  $\text{Ca}(\text{OH})_2$ , in  $\text{CO}_2$  gasification of brown coal and char, even at loadings below 1%. It was signified that use of catalyst lowered the isothermal gasification temperature by 120 K. Lahijani et al. [8] also investigated the effect of some iron species on enhancing the gasification reactivity of palm shell char and found the catalytic effect of them in the order of  $\text{Fe}(\text{NO}_3)_3 > \text{FeCl}_3 > \text{FeSO}_4$ . In another investigation, Kodama et al. [82] simply mixed the metal oxide powders of  $\text{In}_2\text{O}_3$ ,  $\text{ZnO}$  and  $\text{Fe}_2\text{O}_3$  with the ground bituminous coal and studied the effects of these metal oxides on the promotion of the char reaction rate. It was found that the gasification reactivity followed the order of  $\text{In}_2\text{O}_3 > \text{ZnO} > \text{Fe}_2\text{O}_3$  at high temperatures above 850 °C; the reaction rate constant at 900 °C enhanced by 4.9, 2.3 and 1.4 times by  $\text{In}_2\text{O}_3$ ,  $\text{ZnO}$  and  $\text{Fe}_2\text{O}_3$  catalyst, respectively. However, this sequence changed to  $\text{In}_2\text{O}_3 > \text{Fe}_2\text{O}_3 > \text{ZnO}$  at lower temperatures (825 °C).

Although in many catalyzed Boudouard reactions, alkali metals performed better than alkaline earth and transition metals [73,74,83], however, this might not be considered as a general pattern, because the type of carbon char and its physicochemical properties also play a decisive role in the gasification rate. Lahijani et al. [84] studied the effect of nitrate salts on the gasification reactivity of pistachio shell char. The catalytic effect of the salts were found to be in the order of  $\text{NaNO}_3 > \text{Ca}(\text{NO}_3)_2 > \text{Fe}(\text{NO}_3)_3 > \text{KNO}_3 > \text{Mg}(\text{NO}_3)_2$ . In spite of many works, they observed the almost insignificant role of potassium on promoting the char reactivity. Such deviated behavior of K was deduced to be attributed to the increased sintering tendency of biomass ash in the presence of K at high temperatures. As the pistachio shell ash inherently contained a relatively high amount of K, addition of  $\text{KNO}_3$  as catalyst could deteriorate the sintering tendency of ash particles through the formation of low melting eutectics. It was explained that under the gasification condition, the damaging effect of K was against its catalytic effect; as a result the char reactivity could be only slightly improved. Very similar trend was reported by Sun et al. [85] who investigated the  $\text{CO}_2$  gasification reaction rate of marcel chars in the presence of several nitrate catalysts and found the catalytic effect in the sequence of  $\text{NaNO}_3 > \text{Ca}(\text{NO}_3)_2 > \text{Fe}(\text{NO}_3)_3 > \text{KNO}_3$ .

Many efforts have been made to search for effective and cheap catalysts. Black liquor which is the major waste from pulp and paper industry contains a considerable amount of alkaline salts and organic compound which can be used as cheap catalyst to improve the gasification reactivity. In this regard, Zou et al. [86] used black liquor as catalyst in  $\text{CO}_2$  gasification of petroleum coke and investigated the effect of mechanochemical treatments, used to prepare the catalyzed chars, on their gasification reactivity. The effectiveness of the implemented methods followed the sequence of wet grinding > dry grinding > physical impregnation > dry mixing. It was also deduced that in wet grinding method, the active metal species have stronger contact with the char material, thus they are not easily vaporized during the high temperature

gasification and retain their catalytic activity. Similar experiments were performed by Zhan et al. [87]; exactly similar results and discussion was presented by this group of researchers. It was also explained that grinding process led to decrease of the graphitic structure and increase of the specific surface area, where the BET surface area of the samples obtained by grinding was almost ten times that of impregnated or dry mixed samples. In their experiment, the gasification reactivity of black liquor loaded coke was compared to that of  $\text{Na}_2\text{CO}_3$  loaded coke and it was found that the black liquor was more effective in enhancing the reactivity. This is consistent with the work of Valenzuela-Calahorro et al. [88] who reported higher catalytic activity of black liquor compared to NaOH and KOH in  $\text{CO}_2$  gasification. This may be explained by the mechanism of the reaction which involves the formation of some intermediate complexes and then decomposition of them. One of the mechanisms which have been proposed for reduction of alkali compounds with carbon in black liquor catalyzed char can be represented by the following reactions [89,90]:



where M represents the alkali metal and  $[-\text{CO}_2\text{M}]$ ,  $[-\text{COM}]$  and  $[-\text{CM}]$  denote intermediate alkali-surface compounds which react with carbon in the char to produce CO. Valenzuela-Calahorro et al. [88] explained that formation of these active complex with black liquor was higher than NaOH or KOH and that such complexes were more unstable with black liquor. Since the decomposition rate of these complexes is the main factor which controls the rate of gasification of carbon, thus the catalytic activity of black liquor was more profound than NaOH or KOH. In another effort to use cheap catalyst for improving the reactivity of char, Lahijani et al. [91] utilized palm empty fruit bunch ash as a natural catalyst which is rich in potassium to enhance the reactivity of palm shell char in  $\text{CO}_2$  gasification. It was hypothesized that the K in the ash inclined to form intercalation compounds with char carbon matrix, which resulted in volume expansion and weakening of C-C bonds and eventually enhanced the char reactivity. It was also speculated that potassium played a significant role in  $\text{CO}_2$  chemisorption on the catalyzed char and that the potassium site catalyzed the breaking and transfer of oxygen from  $\text{CO}_2$  to the carbon surface and subsequent release of CO.

## 2.2.2. Gasification temperature

It is well understood that char gasification is the slowest step in the conversion of carbonaceous materials to synthesis gas. The conversion rate of char is influenced by a combination of chemical and physical processes which includes: (1) diffusion of the reactant gas ( $\text{CO}_2$ ) from the bulk-gas phase to the surface of carbon (film diffusion), (2) diffusion of  $\text{CO}_2$  into the char particle and its porous structure (pore diffusion), (3) reaction of  $\text{CO}_2$  with carbon on the surface, (4) outward diffusion of the product gas (CO) from the reaction sites and interior of char (pore diffusion) and eventually (5) transfer of CO from the char surface to the bulk-gas phase (film diffusion) [3,10]. Among these steps, only step (3) deals with chemical aspect of the Boudouard reaction and the rest are physical or transport processes. These processes are closely associated with the consequential changes in the pore structure as the Boudouard reaction proceeds and many operational parameters involved in the gasification. Any combination of these processes can control the rate of char conversion.

The gasification temperature is the most significant parameter which affects the gasification reactivity of char and controls the

gasification rate [92]. It is widely understood that at low gasification temperatures the reaction rate is governed by intrinsic (surface) chemical reaction rate; whereas, at high gasification temperatures pore diffusion mechanism becomes dominant and controls the gasification rate [8,93]. It is very common to use an Arrhenius type plot to discriminate between the chemical reaction phase and pore diffusion phase [8,9,14,92,93]. At low gasification temperatures, a linear proportionality can be found between the reaction rate and the inverse temperature in the Arrhenius form which indicates the gasification reaction is chemically controlled. As the gasification temperature is increased, the pore diffusion becomes significantly important. This, leads to a change and decrease in the slope of the Arrhenius plot signifying the shift from chemical reaction regime to pore diffusion regime. In cases where the reaction rate is controlled by diffusion, a good knowledge of the initial char morphology and its porous structure as well as detailed characterization of the char during the gasification is required for evaluating the overall reaction rate [84,93]. Due to the difficulties in use of high temperature data, most gasification experiments are carried out at sufficiently low temperatures to ensure that the reaction rate is governed by surface chemical reaction. To this end, Kim et al. [14] developed an Arrhenius plot for several coal samples gasified under  $\text{CO}_2$  in the temperature range of 1050–1350 °C. They found that at temperatures below 1150 °C the reaction rate was controlled by chemical reaction, while, the pore diffusion found to be the controlling mechanism at temperatures above 1150 °C. Lahijani et al. [84] investigated the effect of temperature on the  $\text{CO}_2$  gasification rate of pistachio shell char in the range of 800–1000 °C. Although high temperature pronouncedly improved the char gasification rate through reducing the activation energy; however, it was hypothesized that use of very high temperature could shift the reaction rate towards pore diffusion controlled regime. When the Arrhenius plot of the average reaction rate was developed, such speculation was confirmed, where three phases (with different slopes) could be observed on the graph. The first phase for temperatures below 875 °C was considered as the chemical reaction regime; the second phase between 875 and 900 °C was considered as the transition phase in which a combination of chemical reaction and pore diffusion resistances could exist, and the third phase for temperatures above 900 °C was found to be the diffusion controlled regime. Such division of gasification reaction rate controlling mechanism was also found in the work of Sinağ et al. [94], while studying the  $\text{CO}_2$  gasification reactivity of lignite char. Yuan et al. [52] also developed the Arrhenius plot based on the gasification rate of some biomass chars to find the region in which the reaction rate is chemically controlled. They reported that the gasification rate was under chemical control regime at temperatures in the range of 850–950 °C and turned to diffusion controlled regime at temperatures above 950 °C. Roberts et al. [9] studied the effect of temperature on the reaction rate of three coal chars in the  $\text{CO}_2$  gasification. At temperatures below 900 °C, intrinsic chemical reaction was found to be the rate controlling mechanism, whereas, at temperatures in the range of 1000–1400 °C, pore diffusion limitations were seen to affect the reaction rate. Based on the developed Arrhenius plots, it was found that the activation energies in the high temperature regime were almost one-half of those calculated in the low temperature condition. Some more discussions regarding the activation energies obtained in the chemical controlled or diffusion controlled regimes are presented in kinetic studies section.

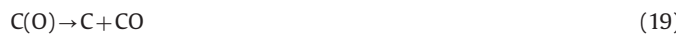
### 2.2.3. Gasification pressure and $\text{CO}_2$ partial pressure

The intrinsic surface reaction rate of char in the gasification reaction is known to be largely independent of total pressure.

However, the rate of diffusion of gas though the pores of char may be influenced by total pressure. Typically, two types of diffusion, namely molecular and Knudsen diffusion, can contribute to the effective diffusivity, where the first one dependent on temperature and total pressure and the second one is only dependent on temperature, but not the total pressure. The molecular diffusion is associated with the diffusion of gas in pores with diameters significantly larger than the mean free path of the gas under the reaction condition; whereas, the Knudsen diffusion is related to the diffusion in pores with diameters smaller than the mean free path of the gas, due to the significant interaction with the walls of the pores [9]. Variation in the total pressure can affect the char reactivity either by changing the partial pressure of the reactant gas or by changing the mass transfer driving force. Malekshahian and Hill [95] investigated the influence of total pressure (0.5–2.4 MPa), at fixed temperature and  $\text{CO}_2$  partial pressure, on the gasification reactivity of petroleum coke. They found the minor influence of total pressure on the reactivity, where the difference between reaction rates was less than  $\pm 20\%$  in the studied pressure range. It was inferred that the insignificant effect of total pressure was consistent with the assumption that the chemical reaction was the rate controlling step and that the reaction was not mass transfer limited. However, in cases where the pressure was changed in the range of 0.1–2.4 MPa with 100%  $\text{CO}_2$ , the reaction rate increased by a factor of 4 between pressures of 0.1 and 2.4 MPa. Such pressure dependence on the gasification rate could be attributed to the number of occupied active sites with increase of the reactive gas pressure. They also presented another work [96] with similar findings and discussion. It was discussed that increase of the  $\text{CO}_2$  partial pressure can shift more catalytic sites to the oxide form and eventually conclude to the increase in the overall reaction rate. Moreover, it was explained that higher pressures suppressed the volatilization and loss of mineral content (mainly potassium) and positively influenced the catalyst distribution; this way the reaction rate could be enhanced at higher pressures. Yet, a different trend was reported by Fermoso et al. [29], where the reactivity of the char at atmospheric pressure (100%  $\text{CO}_2$ ) was higher than that of 10 bar (100%  $\text{CO}_2$ ) at any reaction temperature. This could be explained by increasing mass-transfer limitations and decrease in  $\text{CO}_2$  diffusion at high pressures [95]. However, Fermoso et al. [29] notified that regardless of the total pressure, the reaction rate of char increased with increase of the partial pressure of the reactant gas,  $\text{CO}_2$ . Roberts et al. [9] also reported the increase of coal char reaction rate along with increase of the  $\text{CO}_2$  partial pressure. It was also found that the total pressure had an insignificant effect on the kinetics of the reaction which was consistent with the assumption of the dominance of Knudsen diffusion in the char samples. De Micco et al. [97] investigated the effect of  $\text{CO}_2$  concentration (8–60%) on the gasification reactivity of Rio Turbio coal chars obtained from pyrolysis of coal at 850 and 950 °C. For the char pyrolyzed at 850 °C, the reaction rate increased by increase of the  $\text{CO}_2$  concentration to 30% and a reaction order of 0.5 was obtained with respect to the  $\text{CO}_2$  partial pressure in this case. Nevertheless, for the char pyrolyzed at 950 °C, no influence of  $\text{CO}_2$  concentration on the reaction rate was observed. The reason for such diverse results was somehow discussed in the work of Ahmed and Gupta [98] who investigated the effect of  $\text{CO}_2$  partial pressure on the woodchips char gasification rate. They observed negligible to no changes in the reaction rate along with increase of the  $\text{CO}_2$  partial pressure from 0.6 to 1.5 bar (total pressure was 2.0 bar) which was an indication of a negligible to zero reaction order with respect to the  $\text{CO}_2$  partial pressure in the studied range. It was explained that in a chemically controlled surface reaction, three subsequent processes can take place: (1) chemical adsorption of  $\text{CO}_2$  on the solid surface, (2) surface reaction of  $\text{CO}_2$  with carbon char and

(3) desorption of product, CO, from the solid surface. In cases where the adsorption is the rate controlling step, increase in the partial pressure of CO<sub>2</sub> would improve the reaction rate. However, if the kinetics of the reaction is controlled by the surface reaction or the desorption step, regardless of the concentration of CO<sub>2</sub> above the char surface, there is no vacant active site available for CO<sub>2</sub> adsorption; thereby, any increase in the CO<sub>2</sub> partial pressure would not affect the reaction rate.

Mitsuoka et al. [81] investigated the effect of CO<sub>2</sub> concentration (20–80%) on the gasification rate of Ca-catalyzed char. It was found that at low temperatures, the reaction rate decreased at 80% CO<sub>2</sub>. It was speculated that the retardation of the gasification rate at high CO<sub>2</sub> concentrations was attributed to the inhibition effect imposed by CO, as the product of the gasification. It was explained that CO is disproportionate at catalytic active site to CO<sub>2</sub> and carbon and depress the gasification rate. From thermodynamic view point, the inhibition effect of CO on the char gasification could be overcome at high temperatures. The widely accepted mechanism proposed for CO inhibition is [99]



Frederick et al. [100] studied the effect of CO<sub>2</sub> partial pressure on the gasification rate of black liquor char at 700 °C and 0.8 bar CO partial pressure under a total pressure of 20 bar. The results demonstrated the strong dependence of gasification rate on the CO<sub>2</sub> partial pressure at  $P_{\text{CO}_2} < 15$  bar. However, at high CO<sub>2</sub> partial pressures, the reaction rate became independent of  $P_{\text{CO}_2}$  and the apparent reaction order with respect to CO<sub>2</sub> approached zero, suggesting the saturation of the catalytic active sites at high CO<sub>2</sub> partial pressures. Increase of the total pressure from 1 to 30 bar at fixed gas composition (20% CO<sub>2</sub> and 4% CO) decreased the reaction rate by a factor of 4.6, signifying the strong inhibiting effect of CO.

#### 2.2.4. Char particle size

The size of char particle is one of the influential parameters on the progress of the Boudouard reaction. As the char particle size is reduced, the higher bulk density (larger external surface area/volume) and intraparticle surface area enhances the heat and mass transfer inside the char [101]. Sufficiently small particles are required to ensure that the chemical kinetics is the rate controlling mechanism and that the heat is uniformly distributed throughout the particle [101,102]. In large particle fuels, there might be two limitations which contribute to the lower reaction rate. The first limitation which is considered as physical limitation can be related to diffusional resistances, originating from temperature or CO<sub>2</sub> concentration gradient inside the char particles. The second limitation which is considered as a chemical limitation may originate from inhibition effect imposed by CO; as the gasification reaction takes place to a higher extent the concentration of CO inside the char pores can reach an appreciable level to cause inhibition effect [14,103].

Kim et al. [14] studied the effect of particle size on the reaction rate of two coals, high rank (lower volatile matter, higher ash content) and low rank (higher volatile matter and lower ash content) at different particle sizes of 45, 90, 180 and 274 µm. Although the reactivity of both sample increased with decrease in particle size, however, this effect was less significant for the low rank coal. It was explained that the pore surface area of low rank coal is much larger than the external surface area of the particle, thus, decreasing its particle size slightly influenced the specific surface area, which is related to the pore surface area. Such deduction is consistent with finding of Ergun [28] who reported

that for charcoal and activated graphite, which both were porous, the relative number of active sites per gram was independent of particle size in the range of 80–1800 µm. Mani et al. [104] investigated the influence of particle sizes (60, 250, 638 and 925 µm) on the gasification reactivity of wheat straw char and found that the reactivity decreased as the particle size was increased. In a defined period of time, the highest carbon conversion was achieved with the fine char powder (< 60 µm) implying that the diffusion was limiting the reaction rate for larger char particles. In another investigation conducted by Lee and Kim [66], the gasification reactivity of waste tire char with various particle sizes (250–1200 µm) was studied. The results showed that the reactivity remained almost unchanged with increasing the particle size up to 650 µm and then decreased with further increase of the char particle size. It was speculated that the chemical reaction was the rate controlling mechanism when the particle size was below 650 µm. Gómez-Barea et al. [103] also showed that the CO<sub>2</sub> gasification rate of wood matter from pressed-oil stone was largely influenced by the particle size, where the measured reactivity increased as the particle size decreased from 2100 to 60 µm. It was discussed that in large enough particles, the accumulation of CO inside the particle becomes higher which eventually concludes to the lower reactivity due to the inhibition effect of CO. It was also explained that such condition is exacerbated at high temperatures, wherein, the production of CO is higher.

#### 2.2.5. Gasification heat source

As discussed, the Boudouard reaction is a highly endothermic reaction and high temperatures, typically > 700 °C, are required to shift the equilibrium of the reaction towards CO production. In most carbon-CO<sub>2</sub> gasification studies, such high temperature has been provided by conventional convective heating. However, some works have used solar-driven gasification, wherein, concentrated solar radiation is used to supply the required heat for conversion of carbonaceous material to gaseous fuels through the Boudouard reaction [105,106]. One of the major advantages of solar-driven gasification process is the reduction of net CO<sub>2</sub> emission into the atmosphere, as the process heat is provided by clean renewable solar energy [105,107]. For instance, it has been reported that in solar coal-gasification, almost 26–30% of CO<sub>2</sub> emission can be mitigated compared to the conventional coal gasification [108]. Although solar-driven Boudouard reaction with less CO<sub>2</sub> emission may be considered as a potential alternative to conventional thermal-driven gasification; however, it does not affect the reaction rate of char. Recently, it has been found that microwave-driven CO<sub>2</sub> gasification has an enormous effect on promoting the reaction rate. Hunt et al. [5] reported a remarkable change in the kinetics of microwave-driven CO<sub>2</sub> gasification of activated charcoal, where the apparent activation energy of the reaction dropped from 118 kJ/mol under conventional thermal heating to 38 kJ/mol under microwave irradiation. Such enhancement in the reactivity was hypothesized to arise from the interaction of CO<sub>2</sub> with the electron-hole pairs present at the surface of char due to the space-charge mechanism, which is known to be responsible for heating the char subjected to microwave irradiation. Menéndez et al. [109] compared the CO<sub>2</sub> gasification rate of coffee ground char under microwave and conventional thermal heating and found a great difference between the two heating systems especially at low temperatures. At the gasification temperature of 500 °C, there was no conversion for CO<sub>2</sub> in conventional heating, whereas, the average CO<sub>2</sub> conversion was 88% in microwave. With increase of the temperature this difference reduced to a great extent, where CO<sub>2</sub> conversions of 83% and 100% were achieved at 800 °C for conventional and microwave heating system, respectively. It was discussed that in conventional heating system, the transition

between the controlling mechanisms of the Boudouard reaction, either chemical reaction or diffusion, occurred at 800 °C, however, in microwave driven gasification the reaction was never under pure chemical reaction control. Domínguez et al. [110] also reported that the activation energy for CO<sub>2</sub> gasification of sewage sludge (dry and wet form) in conventional thermal heating system was higher compared to the similar reaction under microwave irradiation. They pointed to the formation of hot-spot, also considered as micro-plasma, inside the char bed under microwave heating which could cause very high temperatures inside the particle and could be responsible for the higher reaction rates.

### 3. Kinetics of char gasification reaction

Studying the kinetics of char gasification provides valuable insight for the appropriate design and operation of gasifiers [8,104]. Knowledge of char gasification rate provides useful information for evaluating the overall gasification process, as it determines the required volume of the gasifier [103]. To appropriately measure the intrinsic reaction rate data, the gasification need to be performed at relatively low temperatures. At this condition, it is most probable that the chemical process controls the gasification rate and the reaction is under chemically or kinetically controlled regime (sometimes referred as "Regime I"). This implies the conditions that the rate of diffusion of reactant gas through the pores of char is negligible in controlling the overall reaction rate and that the reaction mechanism and kinetics can be studied free from physical limitations imposed by diffusion and experimental conditions [9,93]. The kinetic data regarding char-gas reaction obtained under this condition are reliable, accurate and transportable across different reaction conditions. The reaction kinetics under Regime I and the effect of operation parameters such as temperature, reactant gas pressure and char features on the kinetics of char gasification has been well studied.

Although low temperature gasification data have been used to study the kinetics of reactivity of several fuel chars, however, the realistic industrial gasification processes involve temperatures significantly higher than those used in laboratory investigations. For instance, the gasification temperature in Texaco and Shell gasifiers are up to 1700 °C [111]. At high temperature gasification conditions, the rate of diffusion of the reactant gas through the pores of reacting char (typically referred as "Regime II") becomes important. Thus, the kinetic models that are designed to foresee the high temperature char gasification behavior consider the interaction between the rate of surface chemical reaction and the rate of diffusion of reactant into the porous structure of char [93]. Typically, such models have a chemical reaction term which estimates the variation in the intrinsic gasification rate with temperature, reactant gas pressure and carbon (char) type; in combination with a component which considers the diffusional limitations to obtain an overall gasification rate expression for a wide range of temperatures [10]. High temperature gasification reaction requires accurate insight into the microstructure and morphology of char and exact quantification of properties such as particle size and pore size distribution to effectively interpret and analyze the overall gasification rate [9,93]. Due to the difficulties in applying high temperature (Regime II) data, most kinetic studies are performed at sufficiently low temperatures to exclude the diffusional effects in reaction rate controlling mechanism.

The overall gasification reaction rate can be expressed as [97,112–114]

$$r = \frac{dX}{dt} = k(T)G(P_{CO_2})f(X) \quad (20)$$

where  $k(T)$  and  $G(P_{CO_2})$  consider the effects of temperature and CO<sub>2</sub> partial pressure on the reaction rate and  $f(X)$  is a function that describes changes in physicochemical properties of char with reaction degree; indeed, it represents the relationship between reaction rate and carbon conversion. The influence of temperature and CO<sub>2</sub> concentration (partial pressure) on the gasification reaction rate is of particular interest. The quantification of these two parameters is important for application of gasification rate data to a number of practical gasification systems. Generally, two approaches are implemented to represent the dependence of temperature and partial pressure of CO<sub>2</sub>; use of a rate expression obtained from Langmuir–Hinshelwood reaction scheme or use of a global nth-order (power law) reaction rate equation [9].

The global nth-order reaction rate is usually adopted to describe the kinetics of char gasification; it contains variables which are quantifiable and is amenable over a specific range of applications. In this model the dependence of temperature and CO<sub>2</sub> partial pressure on char gasification rate is assumed as

$$k(T)G(P_{CO_2}) = k_0 e^{-E_a/RT} P_{CO_2}^n \quad (21)$$

where the temperature dependence is expressed by Arrhenius equation with  $k_0$  denoting the pre-exponential factor,  $E_a$  representing the activation energy,  $R$  presenting the universal gas constant and  $T$  indicating the absolute gasification temperature. The dependence on CO<sub>2</sub> concentration is given by a power law expression, where  $n$  is the reaction order with respect to CO<sub>2</sub> partial pressure [97]. The pre-exponential factor reflects the effects of carbon crystallinity, catalysis by mineral matters and so forth which are known variables to influence the char-gas reaction, but does not include the effect of surface area [10].

To determine the kinetic parameters and activation energy of the char gasification reaction, two procedures can be used. In the first approach which relies on isoconventional method, apart from  $f(X)$  definition, activation energy is obtained from the slope of the ln  $t$  vs 1/T [97,114]. Since  $f(X)$  is an unknown function, this technique is often regarded as model-free method. To this end, substitution of Eq. (21) in Eq. (20) upon rearrangement yields:

$$\int_0^X \frac{dX}{f(X)} = \int_0^t P_{CO_2}^n k_0 e^{-E_a/RT} dt \quad (22)$$

After integration Eq. (23) is obtained as follows:

$$F(X) = k_0 e^{-E_a/RT} P_{CO_2}^n t \quad (23)$$

Taking logarithm from both sides of Eq. (23) gives

$$\ln t = \ln \left[ \frac{F(X)}{P_{CO_2}^n k_0} \right] + \frac{E_a}{RT} \quad (24)$$

The first term on the right hand side of the above equation is a function of CO<sub>2</sub> partial pressure and degree of reaction. In cases where the partial pressure of CO<sub>2</sub> is constant, the time required to reach a certain reaction degree can be determined as a function of temperature; therefore, Eq. (24) allows for calculation of activation energy from the slope of the linear plot of ln  $t$  vs 1/T, in spite of unknown  $f(X)$  in Eq. (20). This method is typically regarded as model-free analysis.

The second approach, however, determines the reaction rate and kinetic parameters based on a known  $f(X)$  function, assuming that the partial pressure of the gasifying agent remains constant during the gasification. Several kinetic models have been proposed for the term  $f(X)$ , with different formulations. The existing kinetic models can be divided into two categories; theoretical models and semi-empirical models. Well-known theoretical kinetic models for heterogeneous gas-solid reaction which describe the rate of gasification reaction based on the carbon conversion are volume

reaction model (VRM), shrinking core model (SCM), grain model (GM), random pore model (RPM) etc.

The volume reaction model (VRM) or volumetric model assumes that the carbon–gas reaction takes place at the active sites, uniformly distributed throughout the whole char particle, either outside or inside the particle. This model does not consider the structural changes of char during the gasification and presumes that the particle size remains constant as the reaction proceeds, while the particle density reduces [32]. The model is based on the first order reaction as the rate controlling step. In the absence of diffusional resistances, this model leads to the so-called homogeneous model (HM) [38,115,116]. The overall reaction rate is expressed as

$$r = \frac{dX}{dt} = k_{VRM}(1-X) \quad (25)$$

where  $k_{VRM}$  is the first order reaction rate constant and  $X$  represents the carbon/char conversion.

The shrinking core model (SCM) assumes that the reaction initially takes place at the external surface of the char and then proceeds from the surface into the particle and leaves an ash layer behind. Thus, at the intermediate conversion of the solid, there exists an un-reacted core of the char at any time which shrinks over the course of the reaction [113]. The reaction rate based on the SCM, under chemical reaction control is [32]

$$r = \frac{dX}{dt} = \frac{k_{SCM} C^n S_0}{(1-\varepsilon_0)} (1-X)^m \quad (26)$$

where  $k_{SCM}$  is the rate constant of the surface reaction,  $C$  denotes the reactant gas (here  $\text{CO}_2$ ) concentration,  $n$  is the reaction order,  $S_0$  represents the initial reaction surface,  $\varepsilon_0$  is the initial porosity of the particle and  $m$  is a shape factor which depends on the shape of the particle;  $m=2/3$  for spheres,  $m=1/2$  for cylinders and  $m=0$  for flat plates. For  $m=1$  this equation reduced to the VRM. In many cases, with assumption of spherical particle, a simplified form of the SCM is used as

$$r = \frac{dX}{dt} = k_{SCM}(1-X)^{2/3} \quad (27)$$

This simplified form of the SCM is equivalent to the grain model (GM) which assumes that the char particle is composed of small impervious grains which are dispersed in the gas and each grain is converted according to the SCM. In this model, the surface area reduces non-linearly with increase of the reaction degree [117,118]. The rate expression for the GM under chemical reaction control is

$$r = \frac{dX}{dt} = k_{GM}(1-X)^{2/3} \quad (28)$$

where  $k_{GM}$  is the rate constant of the reaction. The above mentioned models are not able to explain the maximum value of the reaction rate after zero conversion [119]. These models predict that the reaction rate will decrease monotonically with conversion, thereby, provide a poor fit for gasification reactions which present a maximum in their rate profiles [95]. The random pore model (RPM) can describe the reaction rate in systems that show a maximum in the rate curve as well as those that show none. This model takes into account the overlapping of pore structure and reduction of the area available for reaction along with progress of the reaction and the carbon burn-off [120]. Under chemical control, the reaction rate is expresses as

$$r = \frac{dX}{dt} = k_{RPM}(1-X)\sqrt{[1-\psi \ln(1-X)]} \quad (29)$$

where  $k_{RPM}$  is the reaction rate constant and  $\psi$  is a structural constant. The maximum that appears in the reactivity curves indicates a geometrical change in the char which is thought to

arise from two counteracting effects, namely, the development of pores and growth of micropores at the initial stage of gasification which contributes to the increase of reaction surface area and the progressive destruction of the pores at their intersections [98,113,121]; the RPM does not consider the formation of any new pore during the gasification reaction [122]. This model contains the parameter  $\psi$ , which is related to the pore structure of unreacted char ( $X=0$ ) and is defined as

$$\psi = \frac{4\pi L_0(1-\varepsilon_0)}{S_0^2} \quad (30)$$

where  $S_0$ ,  $L_0$  and  $\varepsilon_0$  represent the pore surface area, pore length and porosity of the particle, respectively. When  $\psi=0$ , the RPM reduces to the VRM and at  $\psi=1$ , it approaches to the SCM for the cases of  $m \leq 1$  [32]. This way, the RPM is more flexible than the SCM and VRM. Besides the RPM, normal distribution function model (NDM) can also describe the maximum in the reaction rate, even in cases when the maximum is at  $X=0$  [38,119].

Once the experimental conversion degree ( $X$ ) vs time ( $t$ ) plot was fitted to a defined kinetic model, the reaction rate constant ( $k$ ) is obtained, which can then be used in an Arrhenius type equation to give the kinetic parameters, i.e., the activation energy and pre-exponential factor:

$$k = k_0 \exp(-E_a/RT) \quad (31)$$

**Table 1** summarizes a huge amount of works on studying the kinetics of char gasification reaction in the presence of  $\text{CO}_2$  as the gasifying agent. Since, it was desired to summarize as many data as possible on the same basis, some of the data presented in **Table 1** were recalculated, as the units for the gasification temperature, pressure, particle size, activation energy etc. were not the same in different works. In this table, the “intrinsic” or “true” activation energy ( $E^{int}$ ) refers to the cases where the activation energy was measured at sufficiently low temperatures to ensure that the effect of pore diffusion rates was insignificant. In contrast, the “apparent” activation energy ( $E^{app}$ ) was used for cases where the intrinsic reaction phase was not distinctly discriminated from the diffusional phase; the apparent activation energy might include diffusional rates effects [9]. Apart from these definitions and concepts,  $E^{app}$  and  $E^{int}$  in **Table 1** were indicated based on what have been emphasized by the authors of the cited work.

Although RPM is one of the most successful models to describe the char gasification rate; however, this model may not give good results in some conditions. In gasification of various alkali-catalyzed chars and carbons, pronounced rate maximum typically occurs around  $X=0.7$  [32,121]. Therefore, the original RPM which foresees a maximum rate occurring at conversions below 0.393 ( $0 \leq X \leq 0.393$ ) followed by a systematic drop to zero, fails to describe the reactivity profiles of biomass chars with high alkali contents or other alkali-catalyzed chars, wherein the reaction rate increases along with increase of conversion or there exists a maximum at high conversions [121,136]. This unpredicted accelerated reactivity at high conversions might be attributed to an abrupt disintegration of porous char particles into small fractions accompanied by exposure of fresh surface area to the reactant gas [121]. Thus, the general applicability of the RPM yet remained unsatisfactory.

Great deals of researches have been focused on the development of kinetic models which are able to precisely describe the gasification rate curve of char/carbon. To develop a semi-empirical kinetic model able to describe the experimental reaction rate over the entire conversion range, Struis et al. [121] added a new term to the RPM to predict the pronounced acceleration in the reaction rate for  $X > 0.7$ . Their extended kinetic model (ERPM) satisfactorily described a typical reaction rate of pristine wood charcoal, acid-washed charcoal and  $\text{NaNO}_3$  impregnated charcoal over the whole

**Table 1**Kinetic studies on CO<sub>2</sub> gasification of various chars and operation conditions.

| Carbon source                                   | Char type   | Kinetic model                      | T (°C)             | P <sub>tot</sub> (MPa)                                   | Particle size (μm) | Activation energy (kJ/mol)   | Apparatus         | Ref.  |
|---|---|------------------------------------|--------------------|--|--------------------|--|-------------------|-------|
| Carbon black (sterling FT)                      | Li <sub>2</sub> O-char<br>Li <sub>2</sub> CO <sub>3</sub> -char                                 | ln k vs. 1/T                       | 839–1050           | 0.1  | 256                | 93 <sup>aPP</sup><br>201 <sup>int</sup>  | TF                | [3]   |
| Fir wood  | Pure char   | ln r <sub>avg</sub> vs 1/T         | 700–900            | 0.1 (15% CO <sub>2</sub> )                               | < 2000             | 212 (± 8) <sup>aPP</sup>   | TGA               | [121] |
| Waste tire                                      | Pure char   | RPM                                | 850–1000           | 0.1 (20% CO <sub>2</sub> )                               | 150                | 198 <sup>int</sup>   | TB                | [123] |
| Binxian coal                                    | Pure char   | ln R vs 1/T                        | 1000–1300          | 0.1  | 175–355            | 160–180 <sup>aPP</sup>   | TB                | [124] |
| Coal D (high volatile) Coal Y (semi-anthracite) | Pure char   | ln (dX/dt) vs 1/T                  | 840–940            | 0.1–1.0  | 600–1000           | 209–211 <sup>int</sup> (char D)<br>223–250 <sup>int</sup> (char Y)   | TGA               | [125] |
| Coal  | Ce(NO <sub>3</sub> ) <sub>3</sub> -char   | ln (CO, μmol vs 1/T)               | 500–650 or 800–900 | 0.1  | na                 | 71 <sup>aPP</sup> (low temp.) and 140 <sup>aPP</sup> (high temp.)  | TF                | [126] |
| Alkaline black liquor char                      | Pure char   | ln –r <sub>wg</sub> vs 1/T         | 750–850            | 0.1 (95% CO <sub>2</sub> )                               | < 53               | 170–234 <sup>aPP</sup>   | TGA               | [89]  |
| Wheat straw coal                                | Pure char<br>Co-gasified char   | ln R <sub>i</sub> vs 1/T           | 840–950            | 0.1  | 120                | 145 (biomass char)<br>197 (coal char)<br>153 (co-gasified chars)   | TGA               | [61]  |
| Eucalyptus wood                                 | Pure char   | ln r vs 1/T                        | 775–850            | 0.1  | 200                | 230–26 <sup>aPP</sup>  | TGA               | [45]  |
| Grapefruit skin                                 | Pure char   | n.a.                               | 725–800            | 0.1  | na                 | 200–250 <sup>aPP</sup>   | TGA               | [46]  |
| Rice straw (RS) Chinar leaves (CL)              | Pure char   | RPM                                | 850–950            | 0.1  | 56–180             | 203 <sup>aPP</sup> (RS)<br>216 <sup>aPP</sup> (CL)<br>232 <sup>aPP</sup> (PS)  | TGA               | [52]  |
| Pine sawdust (PS)                               |   |                                    |                    |  |                    |  |                   |       |
| Coal  | Pure char   | RPM<br>GM                          | 825–920            | 0.1 (30% CO <sub>2</sub> )                               | < 500              | 166 ± 11 (GM)<br>165 ± 11 (RPM)<br>171 ± 10 (MF)   | DTF               | [97]  |
| Coal Sub-bituminous (SB)                        | Pure char   | In t vs 1/T                        | 900–1060           | 0.1 (50% CO <sub>2</sub> )                               | ≤ 45               | 158 <sup>int</sup> (SB)<br>165 <sup>int</sup> (HVB)  | TGA               | [127] |
| High volatile bituminous (HVB)                  |   | RPM                                |                    |  |                    |  |                   |       |
| Pine  | Pure char   | Power-law f (X) <sup>a</sup>       | 823–873            | 0.1 (50 or 100% CO <sub>2</sub> )                        | 45–63              | 262–263 for both models and both chars   | TGA               | [128] |
| Birch   |   | Three-parameter f (X) <sup>a</sup> | 767–850            |  |                    |  |                   |       |
| Coal  | Pure char   | In k vs 1/T                        | 800–950            | 0.1 (80% CO <sub>2</sub> )                               | 500–1000           | 190 ± 7 <sup>int</sup> (MF)<br>195 ± 13 <sup>int</sup> (GM)  | TGA               | [114] |
| Coal  | Pure char   | RPM                                | 900–1100           | 0.1 (40% CO <sub>2</sub> )                               | 60–79              | 136 (coal)<br>101 (biomass)  | TF                | [62]  |
| Pine sawdust                                    | Co-gasified char  |                                    |                    |  |                    | 138–152 (blends)   |                   |       |
| Petroleum coke                                  | Pure char   | ln r <sub>max</sub> vs 1/T         | 950–1100           | 0.1  | < 74               | 168 (catalyzed char)<br>198 (pure char)  | TGA               | [68]  |
| Brown coal                                      | FeCl <sub>3</sub> -char   | n.a.                               | 800–950            | 0.1 (20% CO <sub>2</sub> )                               | 150–250            | 160 <sup>aPP</sup>   | TF                | [69]  |
| Palm shell                                      | Palm empty fruit bunch  | RPM                                | 800–900            | 0.1  | na                 | 159 <sup>int</sup> (catalyzed char)<br>268 <sup>int</sup> (char)   | TGA               | [91]  |
| ash-char  |   |                                    |                    |  |                    |  |                   |       |
| Pure char                                       |   |                                    |                    |  |                    |  |                   |       |
| Bituminous coal (XYCC)                          | Pure char   | ln r <sub>0.5</sub> vs 1/T         | 1000–1300          | 0.1  | < 125              | 165 <sup>aPP</sup> (XYCC) at T < 1100<br>201 <sup>aPP</sup> (YCCC) at T < 1100<br>92 <sup>aPP</sup> (XYCC) at T > 1100<br>47 <sup>aPP</sup> (YCCC) at T > 1100 | TGA               | [47]  |
| Anthracite coal (YCCC)                          |   |                                    |                    |  |                    | Around 230 <sup>int</sup> for all chars  |                   |       |
| Four Indian coals                               | Pure char   | RPM                                | 800–1080           | 0.1 (pure CO <sub>2</sub> or diluted in N <sub>2</sub> ) | < 150              | Around 230 <sup>int</sup> for all chars  | TGA               | [99]  |
| Flax straw                                      | Pure char   | In k vs 1/T                        | 800–950            | 0.1 (35% CO <sub>2</sub> )                               | 113–1200           | Average 196  | TGA               | [102] |
| Coal SS005 (high volatile)                      | Pure char   | t <sub>0.5</sub> vs 1/T            | 1000–1400          | 0.1 (20% CO <sub>2</sub> )                               | 500–600            | 60 (SS005)<br>200 (SS021)  | FB                | [53]  |
| Coal SS021 (medium volatile)                    |   |                                    |                    |  |                    |  |                   |       |
| Tire  | Pure char<br>3% K <sub>2</sub> CO <sub>3</sub> –char<br>6% K <sub>2</sub> CO <sub>3</sub> –char | VRM                                | 850–1000           | 0.1  | 650                | 239 <sup>aPP</sup> (char)<br>193 <sup>aPP</sup> (3% K <sub>2</sub> CO <sub>3</sub> –C)<br>184 <sup>aPP</sup> (6% K <sub>2</sub> CO <sub>3</sub> –C)            | TB                | [66]  |
| Sewage sludge                                   | Pure char   | In r <sub>0.3</sub> vs 1/T         | 800–900            | 0.1 (30% CO <sub>2</sub> )                               | 1200               | 164 <sup>int</sup>   | FB                | [129] |
| Wood  | Pure char   | In k vs 1/T                        | 900–1100           | 0.1  | na                 | 210 <sup>aPP</sup>   | TF                | [130] |
| 6 types of anthracite                           | Pure char   | SCM                                | 920–1050           | 0.1  | < 100              | 146–202  | TGA               | [39]  |
| Biomass   | Pure char   | VRM                                | 850–1050           | 0.1  | 250–300            | 172 (VRM)<br>142 (SCM)<br>134 (RPM)  | TGA               | [113] |
|   |   | SCM                                |                    |  |                    |  |                   |       |
|   |   | RPM                                |                    |  |                    |  |                   |       |
| Slash pine                                      | Pure char   | VRM                                | 700–800            | 0.1  | 75–106             | 185 <sup>aPP</sup> (P <sub>CO<sub>2</sub></sub> = 1 bar)<br>165 <sup>aPP</sup> (P <sub>CO<sub>2</sub></sub> = 10 bar)  | DTF               | [29]  |
|   |   |                                    |                    | 1.0  |                    |  |                   |       |
| Plastic waste                                   | Pure char   | RPM                                | 925–1025           | 0.1  | na                 | About 250 <sup>int</sup>   | TB                | [48]  |
| Coke  | Pure char   | In k vs 1/T                        | 1000–1200          | 0.1  | 22,000             | 343 (graphite)<br>221 (Ca-graphite)<br>240 (coke)<br>142 (Ca-coke)   | Purpose built TGA | [131] |
| Graphite  | Lime-char   |                                    |                    |  |                    |  |                   |       |
| Petroleum coke                                  | Pure char   | RPM                                | 900–975            | 0.1  | < 90               | 260 ± 24 <sup>int</sup> (P=0.1)<br>254 ± 12 <sup>int</sup> (P=1.4)   | TGA               | [95]  |
| Petroleum coke                                  | Pure char   | NDM <sup>a</sup>                   | 975–1050           | 0.1  | < 125              | 198  | TGA               | [132] |
| Wood  | Pure char at different pyrolysis conditions   | RPM                                | 800–1300           | 0.1  | Very fine          | 216–251 <sup>int</sup> (wood)  | TGA               | [43]  |
| Miscanthus                                      |   |                                    |                    | (33% CO <sub>2</sub> )                                   |                    |  |                   |       |

**Table 1** (continued)

| Carbon source                       | Char type   | Kinetic model   | T (°C)                                    | P <sub>tot</sub> (MPa)                 | Particle size (μm) | Activation energy (kJ/mol)  | Apparatus         | Ref.  |
|-------------------------------------|---|---|---|--|--------------------|---|-------------------|-------|
| Straw                               |   |   |   |  |                    | 177–197 <sup>int</sup><br>(Miscanthus)<br>159–170 <sup>int</sup> (straw)  |                   |       |
| Coal                                | Pure char<br>Ash-free char<br>K <sub>2</sub> CO <sub>3</sub> -ash-free-char | ln [1/t <sub>50</sub> ] vs 1/T  | 650–950                                   | 0.1                                    | < 90               | 135 (char)<br>155 (ash-free char)<br>241 (K <sub>2</sub> CO <sub>3</sub> -ash-free-char)  | TGA               | [75]  |
| Waste tire                          | Pure char   | RPM   | 850–1000                                  | 0.1 (20% CO <sub>2</sub> )             | 150                | 198 <sup>int</sup>  | TB                | [133] |
| Bituminous coal                     | Pure char<br>In <sub>2</sub> O <sub>3</sub> -char                           | HM  | 800–950                                   | 0.1                                    | < 300              | 225 (char)<br>276 (In <sub>2</sub> O <sub>3</sub> -C)<br>270 (ZnO-C)<br>212 (Fe <sub>2</sub> O <sub>3</sub> -C)   | FB                | [82]  |
|                                     | ZnO-char<br>Fe <sub>2</sub> O <sub>3</sub> -char                            |   |   |  |                    |   |                   |       |
| Wood chips                          | Pure char   | ln [(R <sub>0.5</sub> )/P <sup>n</sup> <sub>CO<sub>2</sub></sub> ] vs 1/T | 750–1250                                  | 0.1 (5–100% CO <sub>2</sub> )          | < 300              | 259 (wood chips)  | TB                | [56]  |
| Olive stone                         |   |   |   |  |                    | 201 (Olive stone)   |                   |       |
| Pine seed shell                     |   |   |   |  |                    | 213 (Pine seed shell)   |                   |       |
| Coal                                | Activated carbon  | ln R <sub>0.4</sub> vs 1/T  | 800–1100                                  | 0.1 (30–95% CO <sub>2</sub> )          | na                 | 104–124 <sup>app</sup> (P <sub>CO<sub>2</sub></sub> = 0.31–0.96 atm)  | TGA               | [106] |
| 11 coal samples                     | Pure char   | SCM   | 1050–1400                                 | 0.1                                    | < 250              | 22–136 <sup>app</sup> (T > 1150 °C)<br>125–208 <sup>int</sup><br>(T < 1150 °C)  | TF                | [14]  |
| Petroleum coke                      | Pure char<br>K <sub>2</sub> CO <sub>3</sub> -char                           | ln dX/dt vs 1/T   | 725–825                                   | 0.1                                    | < 90               | 254 ± 21 (char)<br>133 ± 17 (K-char)  | TGA               | [96]  |
| Low rank coals                      |   |   |   |  |                    | 46–86 <sup>app</sup> (LRCs)   |                   |       |
| Medium rank coal                    | Pure char   | SCM   | 1200–1600                                 | 0.1                                    | na                 | 98 <sup>app</sup> (MRC)   | Drop-in-fixed-bed | [92]  |
| High rank coals                     |   |   |   |  |                    | 131–146 <sup>app</sup> (HRCs)   |                   |       |
| Graphite                            |   |   |   |  |                    | 154 <sup>app</sup> (graphite)   |                   |       |
| Refuse-drive fuel                   | Pure char   | ln k vs 1/T   | 700–1000                                  | 0.1                                    | na                 | 221 <sup>app</sup>  | TGA               | [134] |
| Lignite                             | Pure char   | ln k vs 1/T   | 900–980                                   | 0.1                                    | 300–3000           | 146–128 (pyrolyzed at 500–800 °C)   | TF                | [94]  |
| Pistachio shell                     | Pure char   | RPM   | 800–875                                   | 0.1                                    | < 75               | 204 <sup>int</sup> (char)<br>152 <sup>int</sup> (Na-char)   | TF                | [84]  |
| Beech wood chips                    | Pure char   | ln R <sub>50</sub> vs 1/T   | 850–950                                   | 0.1 (10%, 20% or 30% CO <sub>2</sub> ) | 4000–5000          | 154 (for all partial pressures)   | Macro-TGA         | [135] |
| 3 coal samples                      | Pure char   | ln R vs 1/T   | < 900 (intrinsic)<br>1000–1400 (apparent) | 2 (25% CO <sub>2</sub> )               | Na                 | 78 <sup>app</sup> (CRC281)  | PEFR              | [93]  |
|                                     |   |   |   |  |                    | 153 <sup>app</sup> (CRC272)<br>156 <sup>app</sup> (CRC252)<br>242 <sup>int</sup> (CRC281)<br>278 <sup>int</sup> (CRC272)<br>281 <sup>int</sup> (CRC252) |                   |       |
| Commercial steam activated charcoal | Activated charcoal  | ln k vs 1/T   | 813–992 (MH)<br>850–1000 (TH)             | 0.1                                    | 10–300             | 38.5 ± 1.22 (MH)<br>118.4 ± 1.8 (TH)  | MH TH             | [5]   |

n.a.: not available, app: apparent activation energy, int: intrinsic activation energy, TF: tube furnace, DTF: drop tube furnace, FB: fluidized bed, TB: thermobalance, TGA: thermogravimetric analyzer, PEFR: high-pressure entrained flow reactor, MH: microwave heating, TH: thermal heating.

<sup>a</sup> The model has been presented in Table 2.

range of conversion. In another work [137], they used the developed model, ERPM, to predict the gasification behavior of alkali (Na, K), earth-alkali (Ca, Mg) and heavy metal (Zn, Pb, Cu) nitrate impregnated waste wood char; it was shown that the extended model was able to reproduce all the reaction rate data well over the entire conversion range. Duman et al. [22] implemented the ERPM developed by Struis et al. [121,137] to describe the gasification reaction rates of several biomass chars which exhibited a maximum in rate profile at high conversions. Zhang et al. [32] also modified the original RPM and included a new term in it to accommodate the impact of mineral matters or catalyst on the evolution of reaction rate with conversion. The modified RPM (MRPM) was applied for calcium and potassium catalyzed coal char/carbon and the curve fitting results showed that the model could satisfactorily predict the catalyzed char gasification reaction rate profile over the entire range of conversion. Yuan et al. [52] implemented the RPM to describe the gasification rate of rice straw (RS) char, chinar leaves (CL) char and pine sawdust (PS) char, each prepared at three pyrolysis temperatures of 800, 1000 and

1200 °C, in CO<sub>2</sub> gasification. Although in most cases the RPM performed well to describe the reaction rate, however, the fitting results were not good in some conditions. For cases, where the peak value in rate profile appeared at conversions beyond 0.393 (PS char prepared at high temperature), the MRPM developed by Zhang et al. [32,136] gave the best fit to represent the kinetic data. It was deduced that during rapid pyrolysis of this char, melting of particles wrapped some of the alkali matters which were subsequently released as the gasification proceeded and contributed to the high reaction rates at high conversions. Yet, in some cases, the gasification rate profile experienced a maximum in low conversion range, after which, the rate profile decreased sharply and presented trailing phenomenon in the medium-high conversion range (RS and CL chars at low temperatures); the RPM could not represent them well. The reason for such behavior was not clear for Yuan and co-workers; they developed shifted modified RPM (S-MRPM) and used it to describe the gasification reaction rate of chars. Jing et al. [47] used the RPM as well as MRPM and S-MRPM to describe the CO<sub>2</sub> gasification kinetics of several coal chars.

In cases that the gasification rate profile exhibited a maximum in higher or lower conversion range, MRPM and S-MRPM gave better fitting results than the original RPM, suggesting that the gasification was not only affected by the initial pore structure, but also the evolution of pore structure during the gasification and the inherent materials as reflected by the additional parameters involved in the MRPM and S-MRPM. Table 2 summarizes some of the semi-empirical models developed for specific CO<sub>2</sub>-char gasification reactions.

In cases where the overall reaction rate is affected by the partial pressure of CO<sub>2</sub>, well-established Langmuir–Hinshelwood (L–H) type equation, which were developed based on the adsorption and desorption mechanisms, can be used to describe the relation between temperature and pressure as follows [99,139]:

$$k(T)G(P_{CO_2}) = \frac{k_1 P_{CO_2}}{1 + K_2 P_{CO_2} + K_3 P_{CO}} \quad (32)$$

where  $k_1$  is the reaction constant and  $K_2$  and  $K_3$  are the equilibrium adsorption constants of CO<sub>2</sub> and CO, respectively. The

constants  $k_1$ ,  $K_2$  and  $K_3$  are the temperature dependent parameters with Arrhenius type equation [57, 139]. The L–H rate expression may serve to predict both the limitation of the gasification rate at high reactant gas (CO<sub>2</sub>) concentration and the inhibition imposed by the product gas (CO) [29].

Using the L–H equation, the overall gasification reaction rate (Eq. (20)) can be expressed as

$$r = \frac{dX}{dT} = \frac{k_1 P_{CO_2}}{1 + K_2 P_{CO_2} + K_3 P_{CO}} f(X) \quad (33)$$

In an attempt to study the kinetics of the char gasification, Mandapati et al. [99] performed CO<sub>2</sub> gasification of four Indian coal chars at different CO<sub>2</sub> partial pressures. The dependence of the reaction rate on the partial pressure of CO<sub>2</sub> was explained by the L–H model and several kinetic models including VRM, GM and RPM were used to describe the gasification rate of chars based on Eq. (33). Among the three models, the RPM was the most appropriate and versatile model to predict the experimental data. To determine the possibility of any inhibition effect imposed by

**Table 2**  
Some of the semi-empirical models developed to describe the char reaction rate.

| Kinetic model   | Fuel   | T (C)                                       | P <sub>tot</sub> (MPa)      | Model features  | Ref.      |
|---|--|---|-----------------------------|---|-----------|
| $r = \frac{dx}{dt} = r_1 + r_2 + r_3$<br>$r_1 = k_1 \exp(-\xi X^2)$<br>$r_2 = k_2(1-X)$<br>$r_3 = k_3$  | 9 biomass samples  | 750–850                                     | 0.1–3.0                     | The model is comprised of 3 reactions:<br>(1) Catalytic char gasification with deactivation of catalyst.<br>(2) Non-catalytic char gasification.<br>(3) Catalytic char gasification with small amount of stable catalyst.                                     | [138]     |
| $\xi$ is the correlation coefficient and $k$ is the rate constant   |  |   |                             |   |           |
| $r = \frac{dx}{dt} = k(1-X)\sqrt{1-\Psi \ln(1-X)}(1+\theta^p)$<br>$\theta = cX$ or $c(1-X)$   | Ca or K-catalyzed coal char or carbon  | 850   | 0.1                         | (1) The model is based on RPM, called modified RPM (MRPM).<br>(2) The changes in surface area and structure of pores during reaction are controlled by constants $c$ and $p$ .<br>(3) If $c=0$ , the model reduces to the original RPM.                       | [32]      |
| where $\Psi$ is the initial surface parameter<br>and $c$ and $p$ are the empirical constants  |  |   |                             |   |           |
| M-RPM   |  |   |                             |   |           |
| $r = \frac{dx}{dt} = k(1-X)\sqrt{1-\Psi(1-X)}[1+(p+1)(bt)^p]$<br>where $b$ and $p$ are empirical constants and $t$ is the gasification time   | Fir wood charcoal(untreated, acid-washed, NaNO <sub>3</sub> impregnated) and Waste wood char (metal catalyzed) | 750–900                                     | 0.1                         | (1) The model is based on RPM, called extended RPM (ERPM).<br>(2) It describes the pronounced acceleration in the reaction rate for $X > X_{max}$ .   | [121,137] |
| $r = \frac{dx}{dt} = k_0 \exp(-E_a/RT) P_{CO_2}^\nu f(X)$<br>power-law $f(X) f(X) = (1-X)^n$ or three-parameter $f(X)$<br>$f(X) = \text{normfactor} (X+z)^a (1-X)^n$<br>where $a$ , $n$ and $z$ are adjustable parameters and $\nu$ is the reaction order | Pine and birch charcoal  | 823–873 (birch char)<br>767–850 (pine char) | 0.1                         | (1) The models are based on empirical approximation of surface change during the gasification.<br>(2) The models consider a formal reaction order with respect to the CO <sub>2</sub> concentration.  | [128]     |
| $r = \frac{dx}{dt} = k_0 e^{-E_a/RT} P_{CO_2}^n f(X)$<br>$f(X) = (1-X)(aX+b)\exp(-cX^{1/2})$  | Dried sewage sludge char   | 800–900                                     | 0.1 ( $P_{CO_2}$ : 0.1–0.3) | (1) The model is able to reproduce the maximum reactivity at low conversions, $X < 0.2$ .   | [129]     |
| where $a$ , $b$ and $c$ are empirical parameters  |  |   |                             |   |           |
| $r = \frac{dx}{dt} = k(1-X)\sqrt{1-\Psi(1-X)}/[1+(cX)^p]$<br>where $c$ and $p$ are empirical constants  | Rice straw char, chinar leaves char  | 850–1050                                    | 0.1                         | (1) The model is based on RPM, called shifted modified RPM (S-MRPM).<br>(2) It can describe the gasification rate profiles which present a sharp decrease and trailing in the medium-high conversion range.   | [52]      |
| shifted M-RPM   |  |   |                             |   |           |
| $r = \frac{dx}{dt} = r_m \exp\left(-\frac{(X-X_m)^2}{2\omega^2}\right)$<br>where $r_m$ is the maximum gasification rate and $X_m$ is the conversion at maximum gasification rate and $\omega$ is the width of the curve at $r=r_m/2$                      | Petroleum coke   | 975–1050                                    | 0.1                         | (1) This model was named normal distribution function model.<br>(2) The kinetic model is based only one independent variable, $r=f(X)$ . The influence of $T$ and $P$ on the gasification rate is reflected by the variations of the parameters in the model. | [132]     |

CO, as the product of this reaction, gasification was carried out using a mixture of CO and CO<sub>2</sub> and the results were compared to the case where CO<sub>2</sub> was mixed with N<sub>2</sub>. Although the partial pressure of CO<sub>2</sub> in the CO–CO<sub>2</sub> mixture was higher than that of reference test (CO<sub>2</sub>–N<sub>2</sub>), the reaction was relatively slow for the CO–CO<sub>2</sub> mixture signifying the inhibitory effect of CO on the progress of the reaction.

At moderate pressures and while the partial pressure of CO, as inhibiting component, is not very high, the dependency of overall reaction rate on the partial pressure of CO<sub>2</sub> can also be determined using the global nth-order reaction as follows [129]:

$$r = \frac{dX}{dt} = k_0 e^{-E_a/RT} P_{CO_2}^n f(X) \quad (34)$$

where *n* represents the reaction order with respect to the CO<sub>2</sub> partial pressure. This parameter is a useful and practical means to quantify the influence of the partial pressure of the reactant on the gasification rate over defined process conditions [9]. The validity of this equation can be experimentally verified by showing that the order of reaction is neither influenced by temperature nor by the carbon conversion [129]. If applicable, the power rate law model is more desired than the L–H model, as the determination of several kinetic parameters is not required in this rate model and it can be practically integrated into the process models [95].

Lee and Kim [66] studied the kinetics of tire char gasification under varying temperatures and partial pressures of CO<sub>2</sub>. They used some kinetic models to describe the reaction rate, among which, VRM was the best to predict the reaction rate. Upon the obtainment of the reaction rate constant, the plot of ln *k*<sub>VRM</sub> vs *P*<sub>CO<sub>2</sub></sub> was developed, from which the reaction order with respect to CO<sub>2</sub> partial pressure of 0.3–1.0 atm at 950 °C was obtained as 0.68. The gasification reaction rate of tire char with CO<sub>2</sub> was then proposed as *r* = *dX/dt* = 1.49 × 10<sup>8</sup>exp(−57,060/RT)(*P*<sub>CO<sub>2</sub></sub>)<sup>0.68</sup>(1−*X*). Similar kinetic studies were performed by Seo et al. [113] in the CO<sub>2</sub> gasification of biomass char. They used the VRM, SCM and RPM to predict the reaction rate profile; the best fitting results at different temperatures were obtained by the RPM. After determination of the kinetic parameters, the reaction order with respect to CO<sub>2</sub> was obtained from the plot ln *K*<sub>RPM</sub> vs *P*<sub>CO<sub>2</sub></sub> at constant temperature as 0.62. In another investigation undertaken by Murillo et al. [133], kinetics of waste tire char gasification was studied using four kinetic models; namely, VRM, modified VRM, RPM and changing grain size model (CGSM), for which, the reaction order of 0.72, 0.54, 1.0 and 1.0 was obtained, respectively, at fixed gasification temperature of 950 °C and CO<sub>2</sub> partial pressure of 0.2–0.4. Among the implemented kinetic models, the RPM was the best to describe the gasification rate of tire char with a maximum at *X* < 0.4. Thus, the tire char gasification reaction was found to be first order with respect to the CO<sub>2</sub> partial pressure. De Micco et al. [114] applied a power law reaction rate expression in the form of *dX/dt* = *kP*<sub>CO<sub>2</sub></sub><sup>*n* to determine the reaction order in coal CO<sub>2</sub> gasification reaction. For partial pressures up to 61 kPa, an order of about 0.8 was obtained. They declared that the obtained value has no physical sense; however, it is close to a first order reaction with respect to the CO<sub>2</sub> partial pressure which is the order generally assumed for partial pressures below atmospheric pressure.</sup>

Nilsson et al. [129], used the reactivity at the conversion of 0.3, *r*<sub>0.3</sub>, to determine the kinetic parameters and reaction order in the CO<sub>2</sub> gasification of dried sewage sludge char based on the *r*<sub>0.3</sub> = *k*<sub>0</sub>exp(−*E*<sub>a</sub>/RT)(*P*<sub>CO<sub>2</sub></sub>)<sup>*n*</sup>. The plot of *r*<sub>0.3</sub> vs *T* at fixed CO<sub>2</sub> partial pressure of 0.2 and then the plot of *r*<sub>0.3</sub> vs *P*<sub>CO<sub>2</sub></sub> at fixed temperature of 800 °C were used to determine the activation energy and the reaction order. Upon the obtainment of these parameters, an empirical equation was developed for *f*(*X*) to predict the reaction rate based on Eq. (34) at fixed *P*<sub>CO<sub>2</sub></sub> = 0.2 and

the results showed that the model could well represent the experimental data.

#### 4. Concluding remarks

In this paper, the CO<sub>2</sub> gasification of char, from variety of carbon-based materials, was reviewed. The influence of several important parameters on the reaction rate of char during the gasification reaction was considered and different findings and conclusions in the literatures were overviewed. As could be inferred from this review, understanding the relation between char carbon structure and its reactivity during the gasification has become the reason for numerous studies on char surface chemistry. Generally, the reactivity of char in gasification process was found to be dependent on the pore structure of char and its morphology, catalytic activity of the associated ash, the availability of carbon active sites as well as catalytic active sites on the char, thermal history of char during pyrolysis and type of carbon source. Moreover, many operation parameters such as gasification temperature and pressure, CO<sub>2</sub> partial pressure, size of char particle, use of catalyzed char in the reaction and gasification heat source were found to affect the reaction rate of char. It is worth mentioning that many of these factors have a complex effect on the reactivity of the char in CO<sub>2</sub> gasification process. Indeed, it is not always straightforward to distinguish between the promoting and hindering effect contributing to the overall char reactivity, as some of these parameters might change during the course of char gasification. The ultimate achievable conversion of char through the gasification might be a combination of several influential parameters rather than being simply inferred from individual factors.

A great deal of research performed on studying the kinetics of CO<sub>2</sub> gasification of chars, from various carbonaceous materials, was also reviewed in this work. The survey of literature revealed that most kinetic models were presented in terms of the char reaction rate vs char conversion, accommodating the effect of key structural features of char and their evolution during the gasification. However, some kinetic models also considered the effect of CO<sub>2</sub> partial pressure on the evolution of the reaction. It was also found that most kinetic investigations were carried out at sufficiently low temperatures to ensure that the kinetics was controlled by chemical reaction, with insignificant role of diffusion. The effect of char properties and the operation parameters on the char reaction rate could be reflected in activation energy values estimated from kinetic studies.

#### Acknowledgment

The authors gratefully acknowledge the Ministry of Science, Technology and Innovation Malaysia and the Universiti Sains Malaysia for funding this project in the form of Long Term Research Grant Scheme (LRGS) (203/PKT/6723001), USM-ERGS grant (203/PMEKANIK/6730064) and RU Team grant (1001/PJKI-MIA/854001), respectively.

#### References

- [1] Olivier JGI, Greet J-M, Marilena M, Jeroen AHWP. Trends in global CO<sub>2</sub> emissions 2013 report. PBL Netherlands Environmental Assessment Agency; 2013.
- [2] Calo JM, Perkins MT. A heterogeneous surface model for the steady-state kinetics of the Boudouard reaction. Carbon 1987;25:395–407.
- [3] Jalan BP, Rao YK. A study of the rates of catalyzed boudouard reaction. Carbon 1978;16:175–84.

[4] Liu Z, Wang Q, Zou Z, Tan G. Arrhenius parameters determination in non-isothermal conditions for the uncatalyzed gasification of carbon by carbon dioxide. *Thermochim Acta* 2011;512:1–4.

[5] Hunt J, Ferrari A, Lita A, Crosswhite M, Ashley B, Stiegman AE. Microwave-specific enhancement of the carbon–carbon dioxide (boudouard) reaction. *J Phys Chem C* 2013;117:26871–80.

[6] Conway E. Modern aspects of electrochemistry no. 38. New York; 2005.

[7] Weissermel K, Arpe H-J. Industrial organic chemistry. Darmstadt: Wiley; 2008.

[8] Lahijani P, Zainal ZA, Mohamed AR. Catalytic effect of iron species on CO<sub>2</sub> gasification reactivity of oil palm shell char. *Thermochim Acta* 2012;546:24–31.

[9] Roberts DG, Hodge EM, Harris DJ, Stubington JF. Kinetics of char gasification with CO<sub>2</sub> under regime II conditions: effects of temperature, reactant, and total pressure. *Energy Fuels* 2010;24:5300–8.

[10] Roberts DG, Harris DJ. A kinetic analysis of coal char gasification reactions at high pressures. *Energy Fuels* 2006;20:2314–20.

[11] Tay H-L, Li C-Z. Changes in char reactivity and structure during the gasification of a Victorian brown coal: comparison between gasification in O<sub>2</sub> and CO<sub>2</sub>. *Fuel Process Technol* 2010;91:800–4.

[12] Gomez-Barea A, Ollero P, Villanueva A. Diffusional effects in CO<sub>2</sub> gasification experiments with single biomass char particles. 2. Theoretical predictions. *Energy Fuels* 2006;20:2211–22.

[13] Jing X, Wang Z, Zhang Q, Yu Z, Li C, Huang J, et al. Evaluation of CO<sub>2</sub> gasification reactivity of different coal rank chars by physicochemical properties. *Energy Fuels* 2013;27:7287–93.

[14] Kim YT, Seo DK, Hwang J. Study of the effect of coal type and particle size on char–CO<sub>2</sub> gasification via gas analysis. *Energy Fuels* 2011;25:5044–54.

[15] Goyal A, Zabransky RF, Rehmat A. Gasification kinetics of Western Kentucky bituminous coal char. *Ind Eng Chem Res* 1989;28:1767–78.

[16] Asadullah M, Zhang S, Min Z, Yimsiri P, Li C-Z. Effects of biomass char structure on its gasification reactivity. *Bioresour Technol* 2010;101:7935–43.

[17] Min F, Zhang M, Zhang Y, Cao Y, Pan W-P. An experimental investigation into the gasification reactivity and structure of agricultural waste chars. *J Anal Appl Pyrolysis* 2011;92:250–7.

[18] Butterman HC, Castaldi MJ. CO<sub>2</sub> as a carbon neutral fuel source via enhanced biomass gasification. *Environ Sci Technol* 2009;43:9030–7.

[19] Shurtz RC, Fletcher TH. Coal char–CO<sub>2</sub> gasification measurements and modeling in a pressurized flat-flame burner. *Energy Fuels* 2013;27:3022–38.

[20] Scott SA, Davidson JF, Dennis JS, Fennell PS, Hayhurst AN. The rate of gasification by CO<sub>2</sub> of chars from waste. *Proc Combust Inst* 2005;30:2151–9.

[21] Xu K, Hu S, Su S, Xu C, Sun L, Shuai C, et al. Study on char surface active sites and their relationship to gasification reactivity. *Energy Fuels* 2012;27:118–25.

[22] Duman G, Uddin MA, Yanik J. The effect of char properties on gasification reactivity. *Fuel Process Technol* 2014;118:75–81.

[23] Vamvuka D, Karouki E, Sfakiotakis S. Gasification of waste biomass chars by carbon dioxide via thermogravimetry. Part I: Effect of mineral matter *Fuel* 2011;90:1120–7.

[24] Sakawa M, Sakurai Y, Hara Y. Influence of coal characteristics on CO<sub>2</sub> gasification. *Fuel* 1982;61:717–20.

[25] Hurt RH, Sarofim AF, Longwell JP. The role of microporous surface area in the gasification of chars from a sub-bituminous coal. *Fuel* 1991;70:1079–82.

[26] Wu S, Gu J, Li L, Wu Y, Gao J. The reactivity and kinetics of Yanzhou coal chars from elevated pyrolysis temperatures during gasification in steam at 900–1200 °C. *Process Saf Environ Prot* 2006;84:420–8.

[27] Oka S. Fluidized bed combustion. New York: CRC Press; 2010.

[28] Ergun S. Kinetics of the reaction of carbon with carbon dioxide. *J Phys Chem* 1956;60:480–5.

[29] Fermoso J, Stevanov C, Moghtaderi B, Arias B, Pevida C, Plaza MG, et al. High-pressure gasification reactivity of biomass chars produced at different temperatures. *J Anal Appl Pyrolysis* 2009;85:287–93.

[30] González JD, Mondragón F, Espinal JF. Effect of calcium on gasification of carbonaceous materials with CO<sub>2</sub>: a DFT study. *Fuel* 2012;114:199–205.

[31] Molina A, Montoya A, Mondragón F. CO<sub>2</sub> strong chemisorption as an estimate of coal char gasification reactivity. *Fuel* 1999;78:971–7.

[32] Zhang Y, Hara S, Kajitani S, Ashizawa M. Modeling of catalytic gasification kinetics of coal char and carbon. *Fuel* 2010;89:152–7.

[33] Miura K, Hashimoto K, Silveston PL. Factors affecting the reactivity of coal chars during gasification, and indices representing reactivity. *Fuel* 1989;68:1461–75.

[34] Wu H, Yip K, Tian F, Xie Z, Li C-Z. Evolution of char structure during the steam gasification of biochars produced from the pyrolysis of various mallee biomass components. *Ind Eng Chem Res* 2009;48:10431–8.

[35] Kannan MP, Richards GN. Gasification of biomass chars in carbon dioxide: dependence of gasification rate on the indigenous metal content. *Fuel* 1990;69:747–53.

[36] Risnes H, Fjellerup J, Henriksen U, Moilanen A, Norby P, Papadakis K, et al. Calcium addition in straw gasification. *Fuel* 2003;82:641–51.

[37] De Lasa H, Salaises E, Mazumder J, Lucky R. Catalytic steam gasification of biomass: catalysts, thermodynamics and kinetics. *Chem Rev* 2011;111:5404–33.

[38] Jaffri G, Zhang J. Catalytic activity of the black liquor and calcium mixture in CO<sub>2</sub> gasification of Fujian anthracite. *Chin J Chem Eng* 2007;15:670–9.

[39] Zhang L, Huang J, Fang Y, Wang Y. Gasification reactivity and kinetics of typical Chinese anthracite chars with steam and CO<sub>2</sub>. *Energy Fuels* 2006;20:1201–10.

[40] Hattingh BB, Everson RC, Neomagus HWJP, Bunt JR. Assessing the catalytic effect of coal ash constituents on the CO<sub>2</sub> gasification rate of high ash, South African coal. *Fuel Process Technol* 2011;92:2048–54.

[41] Mayer ZA, Apfelbacher A, Hornung A. Effect of sample preparation on the thermal degradation of metal-added biomass. *J Anal Appl Pyrolysis* 2012;94:170–6.

[42] Lahijani P, Zainal ZA, Mohamed AR, Mohammadi M. Co-gasification of tire and biomass for enhancement of tire-char reactivity in CO<sub>2</sub> gasification process. *Bioresour Technol* 2013;138:124–30.

[43] Lin L, Strand M. Investigation of the intrinsic CO<sub>2</sub> gasification kinetics of biomass char at medium to high temperatures. *Appl Energy* 2013;109:220–8.

[44] Keown DM, Li X, Hayashi J-i, Li C-Z. Characterization of the structural features of char from the pyrolysis of cane trash using Fourier transform-Raman spectroscopy. *Energy Fuels* 2007;21:1816–21.

[45] Tancredi N, Cordero T, Rodríguez-Mirasol J, Rodríguez JJ. CO<sub>2</sub> gasification of eucalyptus wood chars. *Fuel* 1996;75:1505–8.

[46] Marquez-Montesinos F, Cordero T, Rodri'guez-Mirasol J. CO<sub>2</sub> and steam gasification of a grapefruit skin char. *Fuel* 2002;81:423–9.

[47] Jing X, Wang Z, Yu Z, Zhang Q, Li C, Fang Y. Experimental and kinetic investigations of CO<sub>2</sub> gasification of fine chars separated from a pilot-scale fluidized-bed gasifier. *Energy Fuels* 2013;27:2422–30.

[48] Gil MV, Fermoso J, Pevida C, Pis JJ, Rubiera F. Intrinsic char reactivity of plastic waste (PET) during CO<sub>2</sub> gasification. *Fuel Process Technol* 2010;91:1776–81.

[49] Di Blasi C. Combustion and gasification rates of lignocellulosic chars. *Prog Energy Combust Sci* 2009;35:121–40.

[50] Yu J, Lucas JA, Wall TF. Formation of the structure of chars during devolatilization of pulverized coal and its thermoproperties: a review. *Prog Energy Combust Sci* 2007;33:135–70.

[51] Chen H, Luo Z, Yang H, Ju F, Zhang S. Pressurized pyrolysis and gasification of Chinese typical coal samples. *Energy Fuels* 2008;22:1136–41.

[52] Yuan S, Chen X-L, Li J, Wang F-C. CO<sub>2</sub> gasification kinetics of biomass char derived from high-temperature rapid pyrolysis. *Energy Fuels* 2011;25:2314–21.

[53] Luo C, Watanabe T, Nakamura M, Uemiya S, Kojima T. Gasification kinetics of coal chars carbonized under rapid and slow heating conditions at elevated temperatures. *J Energy Res Technol* 2001;123:21–6.

[54] Idris SS, Rahman NA, Ismail K, Alias AB, Rashid ZA, Aris MJ. Investigation on thermochemical behaviour of low rank Malaysian coal, oil palm biomass and their blends during pyrolysis via thermogravimetric analysis (TGA). *Bioresour Technol* 2010;101:4584–92.

[55] Vuthaluru H. Investigations into the pyrolytic behaviour of coal/biomass blends using thermogravimetric analysis. *Bioresour Technol* 2004;92:187–95.

[56] Senneca O. Kinetics of pyrolysis, combustion and gasification of three biomass fuels. *Fuel Process Technol* 2007;88:87–97.

[57] Liu G-s Tate AG, Bryant GW, Wall TF. Mathematical modeling of coal char reactivity with CO<sub>2</sub> at high pressures and temperatures. *Fuel* 2000;79:1145–54.

[58] Gonzalo-Tirado C, Jiménez S, Ballester J. Kinetics of CO<sub>2</sub> gasification for coals of different ranks under oxy-combustion conditions. *Combust Flame* 2012;160:411–6.

[59] Brown RC, Liu Q, Norton G. Catalytic effects observed during the co-gasification of coal and switchgrass. *Biomass Bioenergy* 2000;18:499–506.

[60] Habibi R, Kopyscinski J, Masnadi MS, Lam J, Grace JR, Mims CA, et al. Co-gasification of biomass and non-biomass feedstocks: synergistic and inhibition effects of switchgrass mixed with sub-bituminous coal and fluid coke during CO<sub>2</sub> gasification. *Energy Fuels* 2012;27:494–500.

[61] Zhu W, Song W, Lin W. Catalytic gasification of char from co-pyrolysis of coal and biomass. *Fuel Process Technol* 2008;89:890–6.

[62] Jeong HJ, Park SS, Hwang J. Co-gasification of coal–biomass blended char with CO<sub>2</sub> at temperatures of 900–1100 °C. *Fuel* 2014;116:465–70.

[63] Kajitani S, Zhang Y, Umehoto S, Ashizawa M, Hara S. Co-gasification reactivity of coal and woody biomass in high-temperature gasification. *Energy Fuels* 2009;24:145–51.

[64] Portofino S, Donatelli A, Iovane P, Innella C, Civita R, Martino M, et al. Steam gasification of waste tyre: influence of process temperature on yield and product composition. *Waste Manage* 2012;33:672–8.

[65] Straka P, Bučko Z. Co-gasification of a lignite/waste-tyre mixture in a moving bed. *Fuel Process Technol* 2009;90:1202–6.

[66] Lee JS, Kim SD. Gasification kinetics of waste tire-char with CO<sub>2</sub> in a thermobalance reactor. *Energy* 1996;21:343–52.

[67] Haro M, Ruiz B, Andrade M, Mestre AS, Parra JB, Carvalho AP, et al. Dual role of copper on the reactivity of activated carbons from coal and lignocellulosic precursors. *Microporous Mesoporous Mater* 2012;154:68–73.

[68] Zhou Z, Hu Q, Liu X, Yu G, Wang F. Effect of iron species and calcium hydroxide on high-sulfur petroleum coke–CO<sub>2</sub> gasification. *Energy Fuels* 2012;26:1489–95.

[69] Asami K, Sears P, Furimsky E, Ohtsuka Y. Gasification of brown coal and char with carbon dioxide in the presence of finely dispersed iron catalysts. *Fuel Process Technol* 1996;47:139–51.

[70] Karimi A, Gray MR. Effectiveness and mobility of catalysts for gasification of bitumen coke. *Fuel* 2011;90:120–5.

[71] Ohme H, Suzuki T. Mechanisms of CO<sub>2</sub> gasification of carbon catalyzed with group VIII metals. 1. Iron-catalyzed CO<sub>2</sub> gasification. *Energy Fuels* 1996;10:980–7.

[72] Kopyscinski J, Rahman M, Gupta R, Mims CA, Hill JM. K<sub>2</sub>CO<sub>3</sub> catalyzed CO<sub>2</sub> gasification of ash-free coal. Interactions of the catalyst with carbon in N<sub>2</sub> and CO<sub>2</sub> atmosphere. *Fuel* 2014;117:1181–9.

[73] Karimi A, Semagina N, Gray MR. Kinetics of catalytic steam gasification of bitumen coke. *Fuel* 2011;90:1285–91.

[74] Huang Y, Yin X, Wu C, Wang C, Xie J, Zhou Z, et al. Effects of metal catalysts on CO<sub>2</sub> gasification reactivity of biomass char. *Biotechnol Adv* 2009;27:568–72.

[75] Kopyscinski J, Habibi R, Mims CA, Hill JM. K<sub>2</sub>CO<sub>3</sub>-catalyzed CO<sub>2</sub> gasification of ash-free coal: kinetic study. *Energy Fuels* 2013;27:4785–83.

[76] Rao YK, Adjorlolo A, Haberman JH. On the mechanism of catalysis of the Boudouard reaction by alkali-metal compounds. *Carbon* 1982;20:207–12.

[77] Alam M, Debroy T. The effects of CO and CO<sub>2</sub> on the rate of Na<sub>2</sub>CO<sub>3</sub> catalyzed boudouard reaction. *Metall Mater Trans B* 1984;15:400–3.

[78] Quyn DM, Hayashi J-i Li C-Z. Volatilisation of alkali and alkaline earth metallic species during the gasification of a Victorian brown coal in CO<sub>2</sub>. *Fuel Process Technol* 2005;86:1241–51.

[79] Lahijani P, Zainal ZA. Gasification of palm empty fruit bunch in a bubbling fluidized bed: a performance and agglomeration study. *Bioresour Technol* 2010;101:2068–76.

[80] Zhang Y, Ashizawa M, Kajitani S. Calcium loading during the dewatering of wet biomass in kerosene and catalytic activity for subsequent char gasification. *Fuel* 2008;87:3024–30.

[81] Mitsuoka K, Hayashi S, Amano H, Kayahara K, Sasaoka E, Uddin MA. Gasification of woody biomass char with CO<sub>2</sub>: the catalytic effects of K and Ca species on char gasification reactivity. *Fuel Process Technol* 2011;92:26–31.

[82] Kodama T, Funatoh A, Shimizu K, Kitayama Y. Kinetics of metal oxide-catalyzed CO<sub>2</sub> gasification of coal in a fluidized-bed reactor for solar thermochemical process. *Energy Fuels* 2001;15:1200–6.

[83] Kim SK, Park CY, Park JY, Lee S, Rhu JH, Han MH, et al. The kinetic study of catalytic low-rank coal gasification under CO<sub>2</sub> atmosphere using MVRM. *J Ind Eng Chem* 2014;20:356–61.

[84] Lahijani P, Zainal ZA, Mohamed AR, Mohammadi M. CO<sub>2</sub> gasification reactivity of biomass char: catalytic influence of alkali, alkaline earth and transition metal salts. *Bioresour Technol* 2013;144:288–95.

[85] Sun Q, Li W, Chen H, Li B. The CO<sub>2</sub>-gasification and kinetics of Shennu maceral chars with and without catalyst. *Fuel* 2004;83:1787–93.

[86] Zou J, Yang B, Gong K, Wu S, Zhou Z, Wang F, et al. Effect of mechanochemical treatment on petroleum coke–CO<sub>2</sub> gasification. *Fuel* 2008;87:622–7.

[87] Zhan X, Zhou Z, Wang F. Catalytic effect of black liquor on the gasification reactivity of petroleum coke. *Appl Energy* 2010;87:1710–5.

[88] Valenzuela-Calahorro C, Pan YG, Bernalte-Garcia A, Gomez-Serrano V. Thermogravimetric study of anthracite gasification in CO<sub>2</sub> catalyzed by black liquor. *Energy Fuels* 1994;8:348–54.

[89] Gea G, Sánchez JL, Murillo MB, Arauzo J. Kinetics of CO<sub>2</sub> gasification of alkaline black liquor from wheat straw. 2. Evolution of CO<sub>2</sub> reactivity with the solid conversion and influence of temperature on the gasification rate. *Ind Eng Chem Res* 2005;44:6583–90.

[90] Gea G, Murillo MB, Arauzo J. Thermal degradation of alkaline black liquor from straw. Thermogravimetric study. *Ind Eng Chem Res* 2002;41:4714–21.

[91] Lahijani P, Zainal ZA, Mohamed AR, Mohammadi M. Ash of palm empty fruit bunch as a natural catalyst for promoting the CO<sub>2</sub> gasification reactivity of biomass char. *Bioresour Technol* 2013;132:351–5.

[92] Ren L, Yang J, Gao F, Yan J. Laboratory study on gasification reactivity of coals and petcoke in CO<sub>2</sub>/steam at high temperatures. *Energy Fuels* 2013;27:5054–68.

[93] Hodge EM, Roberts DG, Harris DJ, Stubington JF. The significance of char morphology to the analysis of high-temperature char–CO<sub>2</sub> reaction rates. *Energy Fuels* 2009;23:100–7.

[94] Smag A, Sinek K, Tekes A, Misirlioglu Z, Canel M, Wang L. Study on CO<sub>2</sub> gasification reactivity of chars obtained from Soma-Isiklar lignite (Turkey) at various coking temperatures. *Chem Eng Process Process Intensif* 2003;42:1027–31.

[95] Malekshahian M, Hill JM. Kinetic analysis of CO<sub>2</sub> gasification of petroleum coke at high pressures. *Energy Fuels* 2011;25:4043–8.

[96] Malekshahian M, Hill JM. Potassium catalyzed CO<sub>2</sub> gasification of petroleum coke at elevated pressures. *Fuel Process Technol* 2013;113:34–40.

[97] De Micco G, Nasletti A, Bohe AE. Kinetics of the gasification of a Rio Turbio coal under different pyrolysis temperatures. *Fuel* 2012;95:537–43.

[98] Ahmed II AE, Gupta AK. Kinetics of woodchips char gasification with steam and carbon dioxide. *Appl Energy* 2010;88:1613–9.

[99] Mandapati RN, Daggupati S, Mahajani SM, Aghalayam P, Sapru RK, Sharma RK, et al. Experiments and kinetic modeling for CO<sub>2</sub> gasification of Indian coal chars in the context of underground coal gasification. *Ind Eng Chem Res* 2012;51:15041–52.

[100] Frederick WJ, Wag KJ, Hupa MM. Rate and mechanism of black liquor char gasification with carbon dioxide at elevated pressures. *Ind Eng Chem Res* 1993;32:1747–53.

[101] Hernández JJ, Aranda-Almansa G, Bula A. Gasification of biomass wastes in an entrained flow gasifier: effect of the particle size and the residence time. *Fuel Process Technol* 2010;91:681–92.

[102] Mani T, Mahinpey N. Flax straw char–CO<sub>2</sub> gasification kinetics and its inhibition studies with CO. *Can J Chem Eng* 2012.

[103] Gómez-Barea A, Ollero P, Fernández-Baco C. Diffusional effects in CO<sub>2</sub> gasification experiments with single biomass char particles. 1. Experimental investigation. *Energy Fuels* 2006;20:2202–10.

[104] Mani T, Mahinpey N, Murugan P. Reaction kinetics and mass transfer studies of biomass char gasification with CO<sub>2</sub>. *Chem Eng Sci* 2011;66:36–41.

[105] Gokon N, Ono R, Hatamachi T, Liuyun L, Kim H-J, Kodama T. CO<sub>2</sub> gasification of coal cokes using internally circulating fluidized bed reactor by concentrated Xe-light irradiation for solar gasification. *Int J Hydrogen Energy* 2012;37:12128–37.

[106] Ono H, Yoshida S, Nezuka M, Sano T, Tsuji M, Tamaura Y. Kinetics and simulation on a high-temperature solar thermochemical energy conversion process on the Boudouard reaction. *Energy Fuels* 1999;13:579–84.

[107] Piatkowski N, Wieckert C, Weimer AW, Steinfeld A. Solar-driven gasification of carbonaceous feedstock—a review. *Energy Environ Sci* 2011;4:73–82.

[108] Kodama T, Aoki A, Ohtake H, Funatoh A, Shimizu T, Kitayama Y. Thermochemical CO<sub>2</sub> gasification of coal using a reactive coal–In<sub>2</sub>O<sub>3</sub> system. *Energy Fuels* 2000;14:202–11.

[109] Menéndez J, Domínguez A, Fernández Y, Pis J. Evidence of self-gasification during the microwave-induced pyrolysis of coffee hulls. *Energy Fuels* 2007;21:373–8.

[110] Domínguez A, Fernández Y, Fidalgo B, Pis J, Menéndez J. Bio-syngas production with low concentrations of CO<sub>2</sub> and CH<sub>4</sub> from microwave-induced pyrolysis of wet and dried sewage sludge. *Chemosphere* 2008;70:397–403.

[111] Ma Z, Bai J, Li W, Bai Z, Kong L. Mineral transformation in char and its effect on coal char gasification reactivity at high temperatures, Part 1: Mineral transformation in char. *Energy Fuels* 2013;27:4545–54.

[112] Li P, Yu Q, Xie H, Qin Q, Wang K. CO<sub>2</sub> gasification rate analysis of Datong coal using slag granules as heat carrier-for heat recovery from blast furnace slag by using a chemical reaction. *Energy Fuels* 2013;27:4810–7.

[113] Seo DK, Lee SK, Kang MW, Hwang J, Yu T-U. Gasification reactivity of biomass chars with CO<sub>2</sub>. *Biomass Bioenergy* 2010;34:1946–53.

[114] De Micco G, Fouga GG, Bohé AE. Coal gasification studies applied to H<sub>2</sub> production. *Int J Hydrogen Energy* 2010;35:6012–8.

[115] Sawettaporn S, Bunyakiat K, Kitiyanan B. CO<sub>2</sub> gasification of Thai coal chars: kinetics and reactivity studies. *Korean J Chem Eng* 2009;26:1009–15.

[116] Doraiswamy LK, Vigil D, Uner D. Chemical reaction engineering: beyond the fundamentals. New York: CRC Press; 2013.

[117] Irfan MF, Usman MR, Kusakabe K. Coal gasification in CO<sub>2</sub> atmosphere and its kinetics since 1948: a brief review. *Energy* 2011;36:12–40.

[118] Heesink ABM, Prins W, Van Swaaij WPM. A grain size distribution model for non-catalytic gas–solid reactions. *Chem Eng J* 1993;53:25–37.

[119] Silbermann R, Gomez A, Gates I, Mahinpey N. Kinetic studies of a novel CO<sub>2</sub> gasification method using coal from deep unmineable seams. *Ind Eng Chem Res* 2013;52:14787–97.

[120] Liu H, Luo C, Kaneko M, Kato S, Kojima T. Unification of gasification kinetics of char in CO<sub>2</sub> at elevated temperatures with a modified random pore model. *Energy Fuels* 2003;17:961–70.

[121] Struijs RPJ, Von Scala C, Stucki S, Prins R. Gasification reactivity of charcoal with CO<sub>2</sub>. Part I: Conversion and structural phenomena. *Chem Eng Sci* 2002;57:3581–92.

[122] Morimoto T, Ochiai T, Wasaka S, Oda H. Modeling on pore variation of coal chars during CO<sub>2</sub> gasification associated with their submicropores and closed pores. *Energy Fuels* 2006;20:353–8.

[123] Murillo R, Navarro MV, López JM, García T, Callén MS, Aylón E, et al. Activation of pyrolytic tire char with CO<sub>2</sub>: kinetic study. *J Anal Appl Pyrolysis* 2004;71:945–57.

[124] Liu T-f, Fang Y-t, Wang Y. An experimental investigation into the gasification reactivity of chars prepared at high temperatures. *Fuel* 2008;87:460–6.

[125] Roberts DG, Harris DJ. Char gasification with O<sub>2</sub>, CO<sub>2</sub>, and H<sub>2</sub>O: effects of pressure on intrinsic reaction kinetics. *Energy Fuels* 2000;14:483–9.

[126] Suzuki T, Nakajima S, Watanabe Y. Catalytic activity of rare earth compounds for the steam and carbon dioxide gasification of coal. *Energy Fuels* 1988;2:848–53.

[127] Ochoa J, Cassanello MC, Bonelli PR, Cukierman AL. CO<sub>2</sub> gasification of Argentinean coal chars: a kinetic characterization. *Fuel Process Technol* 2001;74:161–76.

[128] Khalil R, Várhelygi G, Jäschke S, Grønli MG, Hustad J. CO<sub>2</sub> gasification of biomass chars: a kinetic study. *Energy Fuels* 2008;23:94–100.

[129] Nilsson S, Gómez-Barea A, Cano DF. Gasification reactivity of char from dried sewage sludge in a fluidized bed. *Fuel* 2012;92:346–53.

[130] Standish N, Tanjung AFA. Gasification of single wood charcoal particles in CO<sub>2</sub>. *Fuel* 1988;67:666–72.

[131] Moon J, Sahajwalla V. Investigation into the role of the boudouard reaction in self-reducing iron oxide and carbon briquettes. *Metall Mater Trans B* 2006;37:215–21.

[132] Zou JH, Zhou ZJ, Wang FC, Zhang W, Dai ZH, Liu HF, et al. Modeling reaction kinetics of petroleum coke gasification with CO<sub>2</sub>. *Chem Eng Process Process Intensif* 2007;46:630–6.

[133] Murillo R, Navarro MV, López JM, Aylón E, Callén MS, García T, et al. Kinetic model comparison for waste tire char reaction with CO<sub>2</sub>. *Ind Eng Chem Res* 2004;43:7768–73.

[134] Cozzani V. Reactivity in oxygen and carbon dioxide of char formed in the pyrolysis of refuse-derived fuel. *Ind Eng Chem Res* 2000;39:864–72.

[135] Guizani C, Escudero Sanz FJ, Salvador S. The gasification reactivity of high-heating-rate chars in single and mixed atmospheres of H<sub>2</sub>O and CO<sub>2</sub>. *Fuel* 2013;108:812–23.

[136] Zhang Y, Ashizawa M, Kajitani S, Miura K. Proposal of a semi-empirical kinetic model to reconcile with gasification reactivity profiles of biomass chars. *Fuel* 2008;87:475–81.

[137] Struijs RPJ, von Scala C, Stucki S, Prins R. Gasification reactivity of charcoal with CO<sub>2</sub>. Part II: metal catalysis as a function of conversion. *Chem Eng Sci* 2002;57:3593–602.

[138] Umeki K, Moilanen A, Gómez-Barea A, Konttinen J. A model of biomass char gasification describing the change in catalytic activity of ash. *Chem Eng J* 2012;207–208:616–24.

[139] Umemoto S, Kajitani S, Hara S. Modeling of coal char gasification in coexistence of CO<sub>2</sub> and H<sub>2</sub>O considering sharing of active sites. *Fuel* 2011;103:14–21.